Spin diffusion across an organic-semiconductor interface

Lucas Goehring*

Department of Physics and Astronomy, University of British Columbia

6224 Agricultural Road, Vancouver,

British Columbia, Canada, V6T 1Z1

(Dated: April 23, 2002)

Abstract

Cross-polarization experiments were done to observe and quantify the diffusion of spin polarization between hydrogen nuclei and phosphorus nuclei, at the surface of an indium phosphide powder coated with 4-trifluoromethylbenzylbromine. I report a series of models describing this spin diffusion, and present NMR results confirming predictions of these models. I show that spin diffusion occurs efficiently across this organic-semiconductor interface. I also show how spin polarization can be manipulated with simple pulse programs. This research will be of use in the development of a technique to enhance NMR signals by the optical pumping of semiconductors.

*Electronic address: goehring@physics.ubc.ca

Contents

I. FORWARD

The aim of these experiments is to observe and quantify the diffusion of spin polarization across the interface of a semiconductor and an organic molecule. My primary motivation is to help develop a technique, using optical pumping and spin diffusion, to enhance the NMR signal of both very large biological molecules, and samples available only in very small quantities. Using the stimulation of a properly polarized laser, one can selectively excite particular spin states of electrons within a semiconductor. As these excited electrons return to equilibrium, they may transfer their spin polarization to the semiconductor's nuclei. This can lead to very high spin polarizations within the semiconductor. The subsequent development of my work will involve attempts to transfer this large spin polarization into a biological sample on the surface of the semiconductor.

In reporting the performed experiments, and in their future development, a number of NMR techniques will need to be explained. After a brief introduction to Nuclear Magnetic Resonance, I shall discuss the general theory of cross-polarization, spin diffusion, magic angle spinning and optical pumping in the first section. In the second section I will develop the specific theory associated with my work, presenting some simple diffusion models. Then, I will summarize my methods, and the experimental apparatus. I shall move on to report and discuss the results of my experiments. I shall conclude with a summary of the observed behavior of spin-diffusion in my samples.

II. INTRODUCTION AND BACKGROUND

A. Nuclear Magnetic Resonance

The techniques of nuclear magnetic resonance (NMR) are used to find detailed descriptions of the structure of matter. Under an external magnetic field, a set of magnetic dipole moments will tend to orient along the magnetic field. This principle has led to a variety of techniques, such as nuclear magnetic resonance (NMR), electron spin resonance (eSR), muon spin resonance (μSR), and magnetic resonance imaging (MRI). In the case of nuclei, the spin of the nucleus produces a magnetic moment, which creates a slight preference for the spin to be either aligned (or sometimes counteraligned) along a magnetic field. Classically, the set of the nuclei can be thought of as having a net magnetization vector, the sum

of countless individual magnetic moments, which points along the magnetic field when in equilibrium. Like a top precessing around a gravitational field, if the magnetization vector is pushed off the external magnetic field axis, it will precess. The spinning magnetization vector will produce electromagnetic waves, which can be measured. The precession frequency depends on the surroundings of the precessing nuclei, and information regarding its chemical environment can be deduced from NMR observations. Both the perturbation from equilibrium, and the measurement of the dipole radiation can be done with a simple radio frequency coil. I shall try to sketch out the necessary concepts. Further discussion on the principles of NMR may be found in specialized textbooks [1] [2].

Now for a bit more detail. A nucleus possesses an angular momentum and a magnetic moment, both arising from the quantum mechanical spin of its components. The magnetic moment $\vec{\mu}$ will be related to the spin, $\vec{I}$, by $\vec{\mu} = \gamma\hbar\vec{I}$. The constant γ is the gyromagnetic ratio, which is different for each nuclear species. Normally, the spin will be aligned randomly in a discrete set of spin states. For example, both hydrogen and phosphorus nuclei have spin 1/2, and so will be in either a +1/2 or -1/2 spin state. Under an external magnetic field, B_0, these spin states will acquire distinct energy levels, with an energy difference between levels of $-\mu B_0$. The magnetic field felt by the nuclei is roughly that of the external field, but it may change slightly depending on the local environment, a phenomenon called chemical shift. If allowed to equilibrate, a large collection of nuclei can be described by a Boltzman distribution. The probability of a single nucleus being in a particular state will then be weighted by the factor $\exp(-E/k_bT)$. Depending on the sign of γ, this implies that there will be a preference for the nuclear spin to be either aligned, or counteraligned with the magnetic field. At room temperature, this will lead to an average magnetization, or spin polarization, on the order of $10^{-6}\hbar$ under a normal NMR field (say 10 Tesla). This may not be much, but for a sample of a few milligrams, this can mean 10^{10} to 10^{15} nuclei can be polarized by the field. Such a large number of individually quantized magnetic moments can be summed up to give a macroscopic magnetization vector, $\vec{M}$, to a sample. For n nuclei

$$\vec{M} = \gamma \sum_{i=1}^{n} \hbar\vec{\mu_i} = \gamma\vec{L}, \tag{1}$$

where $\vec{L}$ is the total spin angular momentum. This magnetization vector is macroscopic, and can be expected to behave classically.

If $\vec{M}$ is not perfectly aligned with $\vec{B}$, it will precess, circling around the magnetic field.

The equation of motion for $\vec{M}$ will be

$$\frac{1}{\gamma}\frac{\partial \vec{M}}{\partial t} = \vec{M} \times \vec{B}. \tag{2}$$

This equation is simply Newton's second law in terms of rotation. The left hand side is the rate of change of the angular momentum vector, while the right hand side is the torque caused by the magnetic field. For a magnetic field in the z axis, equation 2 is solved by

$$\begin{aligned} M_x(t) &= M_0 \sin(\gamma B_0 t), \\ M_y(t) &= M_0 \cos(\gamma B_0 t), \\ M_z(t) &= M_{z0}. \end{aligned} \tag{3}$$

In other words, the magnetization vector orbits the external magnetic field with a frequency, the Larmor frequency, of $\gamma B_0/2\pi$. The changing $\vec{M}$ will radiate electromagnetic waves at this frequency, which can be detected by a very sensitive receiver. By observing the magnetization as a function of time, information about the frequency of the precessing nuclei can be obtained by a fourier transform of the raw data. As each nucleus has a unique Larmor frequency, the observed frequency can describe the composition of the sample. Further, the tiny chemical shifts resulting from the nuclear surroundings are vital for distinguishing different molecules from each other. The chemical shift of hydrogen, for example, can distinguish methane from methanol. In my experiments, the chemical shift of surface phosphorus (bonded to exterior organic molecules), differs from the chemical shift of phosphorus inside of a grain of indium phosphide. Looking at tiny shifts in frequency allows me to follow spin polarization as it diffuses from the surface inwards.

But to observe all this, $\vec{M}$ must be disturbed from equilibrium. This requires some method of manipulating $\vec{M}$. This is done by using a radio frequency transmitter (often the same coil later used as a receiver) to deliver a small rotating electromagnetic field to the nuclei.

Conceptually, the response of a rotating magnetic moment to a rotating electromagnetic field is one of the most difficult ideas of this subject. It can be described in detail, either through the use of analytical mechanics to define the equations of motion in a rotating reference frame, or through the time-dependant perturbation theory of quantum mechanics. Both approaches are mathematically complex, although elegant, and full descriptions are available elsewhere [3] [4]. In simple terms, if we apply an rf field at the same frequency

as the precessing magnetization, then the magnetic field of the rf pulse, and magnetization vector will be moving at the same angular velocity. Let us align the rf field such that its magnetic field $\vec{B_1}$ extends into the xy plane. To $\vec{M}$, this will look like a constant magnetic field in that plane. As it did under the constant field $\vec{B}$, $\vec{M}$ will precess around $\vec{B_1}$. As the rf field is much much weaker than the external field, this motion is both independent of the original precession, and much slower. In the lab frame, $\vec{M}$ will slowly spiral down, as it is moved away from the z axis. If the rf frequency and the Larmor frequency are not matched, then $\vec{B_1}$ and $\vec{M}$ will move relative to each other, and any precession will, over time, average out.

Now we can describe the concept of phase. If we are free to choose a magnetic component of the rf field anywhere in the x-y plane, we can then choose an amplitude and a phase. Let us arbitrarily define a phase of 0 to be along the positive x$'$ axis, in the rotating frame. A 90 degree phase shift would then put $\vec{B_1}$ on the y$'$ axis.

We can now do wonderful things with a simple rf field. For example, first apply a rf pulse just long enough to move $\vec{M}$ into the xy plane. This is called a $\pi/2$ pulse, as $\vec{M}$ rotates by $\pi/2$ radians. Now, if we shift the phase by 90 degrees, $\vec{M}$ and $\vec{B_1}$ are parallel. This is called spin lock, as it can keep $\vec{M}$ stored in the xy plane for long periods of time. Most NMR experiments consist of a series of manipulations of $\vec{M}$ achieved by playing with the rf field. The particular rf pulse sequences I used for this experiment, and a description of what they do, are found in the experimental methods section.

There are two last concepts to introduce here, the spin-lattice relaxation time T_1, and the spin-spin relaxation time T_2. As I mentioned, in equilibrium the magnetization vector is parallel to the external magnetic field. T_1 measures how fast the system returns to this equilibrium. For example, right after a $\pi/2$ pulse there is no component of $\vec{M}$ in the z direction, but over time the magnetization follows the evolution $M_z(t) = M_0(1\text{-}\exp(-t/T_1))$. The return to equilibrium occurs as the nuclei exchange energy with their surroundings, be it through solitons in a solid, thermal excitations and jostling in a liquid, or through intermediaries such as orbiting electrons. During spin lock, this decay occurs at a suppressed rate, $T_{1\rho}$. T_2 relaxation measures how quickly $\vec{M}$ decreases while in the xy plane. As I stated, there are a spread of frequencies in most samples, caused by different chemical shifts. Further, there will be inhomogeneities in B that will cause slight differences in the precession rates across the sample. No matter what the source, this means that $\vec{M}$ is made

up of many vectors with slightly different Larmor frequencies. Thus, $\vec{M}$ will decohere as these different frequencies move away from each other. Over time, this causes the transverse (xy) amplitude of M to decrease, roughly exponentially, to nothing. The time constant in this exponential decay is T_2

Although it is a powerful technique, NMR has some drawbacks. Most important to this work is the size of the sample required to perform any experiments. In cases of large biological molecules, protein for example, getting enough copies of the molecule to see via NMR can be a major problem. The aim of this research is to investigate a possible technique to use spin diffusion from an optically pumped semiconductor to transfer nuclear magnetization into a surface layer.

B. Spin Diffusion

When, for some reason, a sample has an uneven distribution of nuclear magnetization, it may display spin diffusion. This happens when nearby nuclei exchange angular momentum via the dipole-dipole interaction [5]. The spin Hamiltonian [6] of an NMR sample consists of

$$H = -\gamma\hbar B_0 \sum_{j=1}^{N} I_{jz} + \hbar \sum_{i\neq j} B_{ij}(I_{iz}I_{jz}) - \hbar \sum_{i\neq j} \frac{B_{ij}}{4}(I_{i+}I_{j-} + I_{i-}I_{j+})), \tag{4}$$

where B_0 is the applied magnetic field, γ is the gyromagnetic ratio, I_i is the spin of the ith nuclei, and the operator B_{ij} is defined by

$$B_{ij} = \frac{1}{2}\gamma^2\hbar r_{ij}^{-3}(1 - 3\cos^2(\theta_{ij})). \tag{5}$$

Here, r_{ij} is the displacement vector joining nuclei i and j, while θ_{ij} is the angle this vector makes to the external magnetic field. The first term in this Hamiltonian represents the energy of a collection of independent spins in a magnetic field, and leads to the time dependance of equation 2. The second term is a Zeeman term, which accounts for the perturbation of the spin energy from the magnetic field induced by nearby spins. However, these terms contain no means of dynamic spin interaction. It is only the last term, invoking a dipole-dipole interaction, which allows two nearby spins to exchange energy and angular momentum.

Classically, diffusion obeys the heat equation,

$$U_t = D\nabla^2 U, \tag{6}$$

for some diffusion constant D, and density variable U. It turns out that the exchange of spin polarization via the dipole-dipole interaction can be approximated by this simple differential equation. The details and justification are described elsewhere [5] [7], but a plausibility argument can be provided. Let U(x,t) be the spin polarization density at position x and time. Then, based upon the hamiltonian of equation 4, U will evolve by

$$U_t = \frac{i}{\hbar}[U, H]. \tag{7}$$

Comparing equations 6 and 17, one sees that, assuming the approximation is valid, we can find the value of D by

$$D\nabla^2 U \;=\; \frac{i}{\hbar}[U, H]. \tag{8}$$

Now, the evolution of the spin density is equivalent to the evolution of individual spin states, so for a spin I_i

$$\begin{aligned} D\nabla^2 I_i \;&=\; \frac{i}{\hbar}[U, H] \\ &=\; -\frac{i}{\hbar}[I_i, \hbar \sum_{j\neq i} \frac{B_{ij}}{4}(I_{i+}I_{j-} + I_{i-}I_{j+})]. \end{aligned} \tag{9}$$

To proceed further, as a reasonable first guess, we assume that the angle θ_{ij} is randomly distributed. Then

$$< B_{ij} > \;=\; \frac{\gamma^2\hbar}{2r_{ij}} < 1 - 3cos(\theta_{ij}) >= -\frac{\gamma^2\hbar}{4r_{ij}}, \tag{10}$$

$$D\nabla^2 I_i \;=\; \frac{i\hbar\gamma^2}{16r_{ij}^3}[I_i, \sum_{j\neq i} I_{i+}I_{j-} + I_{i-}I_{j+}]. \tag{11}$$

Now, crudely, one can interpret the equation for spin transfer $I_{i+}\, I_{j-} + I_{i-}\, I_{j+}$ as a differential in I, $r_{ij}\frac{\partial}{\partial r_{ij}} I_i$. Acting similarly with the commutator yields an estimate for the diffusion equation of

$$D_{ij} \simeq \frac{\gamma^2\hbar}{16r_{ij}}. \tag{12}$$

This is very bad quantum mechanics, but gives a dimensionally correct estimate. The consideration of the prefactor 1/16 is also somewhat insightful. Equation 12 can be generated on purely dimensional grounds, without this prefactor.

Upon working through the full mathematical treatment of the Hamiltonian of equation 4, the authors of spin diffusion papers came up with similar estimates. Lowe and Gade [5] calculate that, for a bcc simple cubic lattice, to within 50% that

$$D \simeq 0.15\frac{\gamma^2\hbar}{r}, \tag{13}$$

where r is the distance between nearest neighbors. A similar calculation by Redfield and Yu [7] comes up with the estimate

$$D \simeq 0.04\frac{\gamma^2\hbar}{r}. \tag{14}$$

Both these calculations are based on simple cubic lattices. However, other lattice shapes should only introduce small geometric corrections into the diffusion constant.

Let us try find the spin diffusion constant for indium phosphide, the semiconductor used in my experiments. The above estimates are all consistent with each other, and may be summarized in an order of magnitude approximation as D $\simeq 0.1\frac{\gamma^2\hbar}{r}$. Indium phosphide has a gyromagnetic ratio of $1.08{\cdot}10^8$ rad/T s. The spacing between adjacent nuclei can be calculated as 3.7 $\mathring{A}$, given that the density of InP is 4.787 g/cm^3. This gives the best estimate of D, to within a factor of 2 or so, as $3 \cdot 10^{-17}$ m^2/s.

C. Hartmann-Hahn Cross-polarization

How can spin polarization move between nuclei of different species? Not only does angular momentum have to be conserved, but so does energy. The spin states of all nuclei are quantized in units of $\hbar$, but the energy quantization is dependant on the magnetic field. For a given nucleus,

$$\Delta E = \hbar\omega_{larmor} = \hbar\gamma B_0. \tag{15}$$

In order for cross-polarization, where spin polarization can shift between nuclear species, we have to arrange for nuclei with different γ's to have the same energy difference. This is done by the Hartmann-Hahn condition, named for the original researchers who proposed the technique in 1962 [8]. We need to subject the two sets of nuclei to magnetic fields such that

$$\gamma_1 B_1 = \gamma_2 B_2. \tag{16}$$

As the external magnetic field B_0 is fixed, it cannot be used to achieve this condition. This trick is done through two rf fields, each at one of the necessary Larmor frequencies. The rf fields do not interfere with each other, as a precessing nucleus will only respond to an rf field precisely tuned to the precession frequency. The field intensities can be set to the necessary ratio, and spin diffusion can occur exactly as it does between homogeneous nuclei.

Let me go through the general procedure using a preexisting hydrogen magnetization, $\vec{M}_H$ to polarize phosphorus nuclei. $\vec{M}_H$ is initially in the z direction. After a $\pi/2$ pulse, we spin lock one rf frequency on $\vec{M}_H$. It will then be fixed in the x-y plane. Here I should discuss spin lock in a bit more detail. In the rotating reference frame, $\vec{M}_H$ is parallel to what it sees as the constant magnetic field $\vec{B'_H}$, which is in the xy plane. Consider a small perturbation to $\vec{M}_H$, caused through T_2 relaxation. This will cause $\vec{M}_H$ to precess about $\vec{B'_H}$, eventually reaching a point 180 degrees from the original perturbation. But T_2 relaxation occurs when different components of $\vec{M}_H$ precess at different rates. This means that a spin precessing slightly faster than average will, over time, be swung behind the average magnetization. This auto-correction allows the magnetization vector to maintain itself for times much longer than normally allowed by T_2 relaxation. A similar argument can be made for T_1 relaxation. The decay of a spin locked magnetization will follow a time constant known as $T_{1\rho}$.

If there is a second rf field at the phosphorus resonance, it will initially carry along with it no spin polarization. However, when the field intensity is raised to (γ_H/γ_P)B'$_H$, the Hartmann-Hahn condition is satisfied, and spin polarization diffuses freely between hydrogen and phosphorus nuclei.

D. Magic Angle Spinning

In the Hamiltonian discussed for spin diffusion, equation 4, one may note that with a judicious choice in the angle θ_{ij}, the spin hamiltonian reduces to the hamiltonian of a set of non-interacting spins in a magnetic field. This is the 'magic angle' $\theta_{ij} = 54.73^o$ where $3\cos^2(\theta_{ij})$ - $1 = 0$. θ_{ij} represents the angle the magnetic field makes to the vector joining the two spins i and j. If one spins the NMR sample at this magic angle, then the time average of all R_{ij} will be 54.73^o, assuming the sample is spin quickly enough. In effect, this technique is useful if you spin at an angular frequency faster than the dipole broadened width of the resonance. Unfortunately for my experiments, suppression of dipole interactions at the

magic angle also suppresses the interactions causing spin diffusion.

III. THEORY

A. Diffusion Models

In my experiments, I have worked exclusively with observing spin diffusion between a hydrogen reservoir in a thin coating of 4-trifluoromethylbenzylbromine (TFMBB), and a fine grained indium phosphide powder. As I have described, spin diffusion can be modelled effectively by the classical heat (or conduction-diffusion) equation

$$U_t = D\nabla^2 U \tag{17}$$

with diffusion constant D. Investigating the properties of simple diffusion models has provided insight into my results. In this section, I shall describe a series of models, progressing from the trivial to the more complex descriptions of spin diffusion, as they pertain to cross-polarization from a hydrogen surface to an inner phosphorus layer.

In general, I shall only consider diffusion in one direction. On the timescales of up to a few seconds, spin diffusion only occurs over a few tens of angstroms. Thus, the particles may be considered as infinitely 'deep', with interesting effects only happening over a thin surface. In one dimension, equation 17 reduces to

$$U_t = DU_{xx} \tag{18}$$

1. Diffusion from a point source

Consider the situation where polarization is initially concentrated at the surface of a sample, and subsequently diffuses inwards. This may be the case just after cross polarization between the organic surface and the semiconductor has occurred. A brief cross polarization phase may be followed by a much longer delay before acquisition. This evolution can be modelled by the set of equations

$$\begin{gathered} U_t = DU_{xx}, \ \ -\infty < x < \infty, \ t \geq 0, \\ \text{U bounded as } \mid x \mid \rightarrow \infty, \ U(x,0) = \delta(x), \end{gathered} \tag{19}$$

where U(x,t) represents the spin polarization density at a point. I have extended the domain from 0 to $-\infty$ by noting that the boundary conditions (BC) for U should be $U_x(0,t) = 0$. As the initial conditions are symmetric about x=0, the BC continue to be satisfied through this extension. This is analogous to the method of imaging used in electromagnetics. These equations can be solved via Fourier transforms, where

$$\begin{aligned} V(k,t) &= \frac{1}{2\pi}\int_{-\infty}^{\infty} U(x,t)e^{-ikx}dx, \\ V_t(k,t) &= -Dk^2V(k,t),\ V(k,0) = \frac{1}{2\pi}. \end{aligned} \tag{20}$$

To satisfy the initial condition, and the BC's at infinity, the solution for V is

$$V(k,t) = \frac{1}{2\pi}e^{-Dk^2t}, \tag{21}$$

which corresponds to the gaussian solution for U of

$$U(x,t) = \frac{1}{\sqrt{4\pi Dt}}e^{-x^2/4Dt}. \tag{22}$$

Of particular interest, here, is the average distance travelled by the diffusing spin polarization. The flow of spin polarization away from the surface should be detectable as a slight time dependant change in the chemical shift of the phosphorus signal. It will also give a measure of the volume of a semiconductor involved in the spin diffusion process. When experiments are done in the reverse direction, and spin polarization is moved from a semiconductor into a surface molecule, this is of importance. The mean value of U in this model is simply

$$X(t) =< U(x,t) >= \frac{\int_0^{\infty} xe^{x^2/4Dt}dx}{\int_0^{\infty} e^{x^2/4Dt}dx} = \sqrt{4Dt/\pi}. \tag{23}$$

For perspective, with a diffusion constant of 10^{-17} m^2/s, it will take 0.025 s for spin polarization to diffuse an average of 5Å, and 20 s to diffuse 140Å.

2. Diffusion from a constant source

While the hydrogen polarization is in contact with the phosphorus via cross-polarization (and vice-versa), a different model is appropriate. Initially, we can approximate the source as having a constant spin polarization density, implying a constant spin temperature, and have this polarization move into an initially empty region. This does not conserve the total

spin polarization in the system, but is a realistic model for very short cross polarization times. If we assume that only the surface molecule of organic material contributes spin, we have an initial spin polarization in only a few Å. The previous model suggests that for times of only a few ms, this is a realistic approach. As we shall later see, it is in fact the short $T_{1\rho}$ of the surface hydrogen that will account for the limited accuracy of this model when analyzing my experiments.

Consider the system described by the equations

$$\begin{aligned} U_t = DU_{xx},\ 0 < x < \infty,\ t \geq 0, \\ \text{U bounded as } x \to \infty,\ U(x,0) = 0,\ U(0,t) = U_0. \end{aligned} \tag{24}$$

Where the term U_0 is proportional to the spin polarization density of the source, and D is the diffusion constant. This can be solved with Laplace transforms:

$$\begin{aligned} V(x,s) = \int_0^\infty U(x,t)e^{-st}dt. \\ sV(x,s) = DV_{xx}(x,s),\ V(0,s) = \frac{U_0}{s}, \end{aligned} \tag{25}$$

which has the solution, when the BC at infinity are considered, of

$$V(x,s) = \frac{U_0}{s}e^{-x\sqrt{s/D}}. \tag{26}$$

Taking the inverse Laplace transforms yields the equation

$$U(x,t) = U_0 \text{Erfc}(\frac{x}{2\sqrt{Dt}}) = \frac{2U_0}{\sqrt{\pi}} \int_{x/2\sqrt{Dt}}^\infty e^{-\lambda^2} d\lambda. \tag{27}$$

With this model, we can calculate the total spin polarization that has crossed the boundary as a function of time – a measurable quantity that is of some importance. If η(t) represents the total polarization in the phosphorus, then by integrating,

$$\begin{aligned} \eta(t) &= \frac{2U_0}{\sqrt{\pi}} \int_0^\infty \int_{x/2\sqrt{Dt}}^\infty e^{-\lambda^2} d\lambda dx \\ &= \frac{2U_0}{\sqrt{\pi}} \int_0^\infty \int_1^\infty \frac{x}{2\sqrt{dt}} e^{-\lambda'^2 x^2/4Dt} d\lambda' dx \end{aligned} \tag{28}$$

where I have made the change of variable $\lambda = \frac{x}{2\sqrt{Dt}}\lambda'$. Upon switching the order of integration,

$$\eta(t) = \frac{2U_0}{\sqrt{\pi}} \int_1^\infty \int_0^\infty \frac{x}{2\sqrt{Dt}} e^{-\lambda'^2 x^2/4Dt} dx d\lambda' = \frac{2U_0\sqrt{Dt}}{\sqrt{\pi}} \int_1^\infty \frac{1}{\lambda'^2} d\lambda' = U_0\sqrt{\frac{4Dt}{\pi}} \tag{29}$$

You may note that this is the same function as the average distance found in the previous model, apart from a scaling factor that accounts for the spin density of the source.

3. Diffusion from a decaying source

As I mentioned, the failure of the previous model to fully describe these experiments is mainly due to a short $T_{1\rho}$ in the proton spin reservoir . A slightly modified model can take this decay of the source into account:

$$\begin{aligned} U_t = DU_{xx},\ 0 < x < \infty,\ t \geq 0, \\ \text{U bounded as } x \to \infty,\ U(x,0) = 0,\ U(0,t) = U_0 e^{-t/\tau}. \end{aligned} \tag{30}$$

Again, we can solve this using Laplace transforms. This gives the s-space representation

$$V(x,s) = \frac{U_0}{s + 1/\tau} e^{-x\sqrt{s/D}}. \tag{31}$$

Using the convolution theorem for Laplace transforms, this yields

$$U(x,t) = U_0 \int_0^t \frac{x}{2\lambda\sqrt{\pi\lambda D}} e^{-(t-\lambda)/\tau} e^{-x^2/4D\lambda} d\lambda, \tag{32}$$

a truly terrifying proposition. Fortunately the total polarization that has diffused into the sample, $\eta(t)$ reduces to a simpler form.

$$\begin{aligned} \eta(t) &= U_0 \int_0^\infty \int_0^t \frac{x}{2\lambda\sqrt{\pi\lambda D}} e^{-(t-\lambda)/\tau} e^{-x^2/4D\lambda} d\lambda dx \\ &= U_0 \int_0^t \frac{1}{2\lambda\sqrt{\pi\lambda D}} e^{-(t-\lambda)/\tau} \int_0^\infty x e^{-x^2/4D\lambda} dx d\lambda \\ &= U_0 \int_0^t \frac{1}{2\lambda\sqrt{\pi\lambda D}} e^{-(t-\lambda)/\tau} 2D\lambda d\lambda \\ &= U_0 \sqrt{\frac{D}{\pi}} e^{-t/\tau} \int_0^t \frac{1}{\sqrt{\lambda}} e^{\lambda/\tau} d\lambda \\ &= \sqrt{\frac{4D\tau}{\pi}} e^{-t/\tau} \int_0^{\sqrt{t/\tau}} e^{\lambda'^2} d\lambda'. \end{aligned} \tag{33}$$

For short times, further simplification can be made. By a change of variables, the above integral representation becomes

$$\begin{aligned}
\eta(t) &= U_0\sqrt{\frac{4Dt}{\pi}}e^{-t/\tau}\int_0^1 e^{t\sigma^2/\tau}d\sigma \\
&= U_0\sqrt{\frac{4Dt}{\pi}}e^{-t/\tau}\int_0^1 1+\frac{t\sigma^2}{\tau}+\frac{t^2\sigma^4}{2\tau^2}+...d\sigma \\
&= U_0\sqrt{\frac{4Dt}{\pi}}e^{-t/\tau}(1+\frac{1}{3}\frac{t}{\tau}+\frac{1}{2\cdot 5}\frac{t^2}{\tau^2}+...) \\
&= U_0\sqrt{\frac{4Dt}{\pi}}e^{-t/\tau}(e^{t/3\tau}+\frac{2}{45}\frac{t^2}{\tau^2}+...) \\
&\simeq U_0\sqrt{\frac{4Dt}{\pi}}e^{-2t/3\tau}, \qquad (34)
\end{aligned}$$

where the 2nd order corrections reach only 3 % of the solution when $t = \tau$. In the region where $t < \tau$, this is a good approximation. I use this equation to describe the flow of spin polarization from an organic surface layer into a semiconductor. Unfortunately, the approximations made, namely in choosing an infinitely deep boundary condition, and assuming that the relaxation rate of the destination nuclei is much less than that of the source, do not easily allow this solution to be applied to the reverse experiment of spin polarization diffusing from the semiconductor into the thin organic surface.

4. A numerical simulation

The previous result has reached the limit of my skills as a mathematician. Further complications on the basic diffusion calculation render the calculations so difficult that I cannot solve them analytically. Yet, there are a number of unsavory assumptions built into my models that can significantly change the model behavior. Two are worth considering further. First, with the given boundary conditions, the total spin polarization is not conserved. As much polarization as is required can flow across the boundary at x=0. If there were a limited store of spin polarization in the system, then we need to somehow include that in the calculations. Further, if there is only a limited amount of spin polarization in the boundary, then moving it back and forth across x=0 should change the boundary intensity – the decay would no longer be purely exponential, but would include a drain or source term depending on the polarization density at x=0.

Both these difficulties can be overcome through a numerical simulation of what I best understand to be the dynamics of my samples. A thin reservoir, in which both diffusion and $T_{1\rho}$ relaxation occur, models the hydrogen surface layer. It is linked to a very deep, initially vacant, diffusive body, representing the phosphorus nuclei in the InP. In mathematical terms, I want to numerically solve

$$U_t = \{^{DU_{xx}-U/T_{1\rho} \text{ if x} < \text{x}_0}_{DU_{xx} \text{ if x} > \text{x}_0} \tag{35}$$

for the domain $[0, \infty]$, with an insulating boundary condition at x=0, and an initial condition where U is constant on $0 < x < x_0$, and 0 elsewhere.

To do this, I used Excel to calculate the discrete form of equation 35, where

$$\begin{aligned} U_{0,t+1} &= U_{0,t} - \frac{\Delta t}{T_{1\rho}} U_{0,t} + \frac{D\Delta t}{\Delta x^2}(U_{x+1,t} - U_{x,t}) \\ U_{x,t+1} &= U_{x,t} - \frac{\Delta t}{T_{1\rho}} U_{x,t} + \frac{D\Delta t}{\Delta x^2}(U_{x-1,t} - 2U_{x,t} + U_{x+1,t}),\ 1 < \text{x} < 20 \\ U_{x,t+1} &= U_{x,t} + \frac{D\Delta t}{\Delta x^2}(U_{x-1,t} - 2U_{x,t} + U_{x+1,t}),\ 20 \leq \text{x} < 200. \end{aligned} \tag{36}$$

As initial conditions, I set $U_{x,0}$ to 1 for $0 \leq \text{x} < 20$, and to 0 elsewhere. My step sizes were $\Delta\text{x} = 0.2$ Å, $\Delta\text{t} = 5$ μs. This corresponds to a 4 Å hydrogen source layer and a 36 Å InP layer. I used the diffusion constant $\text{D} = 3{\cdot}10^{-17}$ m^2/s, and a $T_{1\rho}$ relaxation rate of 10 ms. I ran this simulation up to 30 ms.

First, to check that only negligible amounts of spin polarization were escaping out of the open phosphorus boundary, and to see what the distribution of spin polarization might look like, I looked at the spin density as a function of x, at t = 5, 10, and 25 ms. These are shown in figure 1. The maximum spin polarization in the phosphorus reaches about a third of the total initial spin polarization.

Now, as a test of the validity of the previous model, I plotted

$$U(t) = \frac{1}{2\Delta x}\sqrt{\frac{4Dt}{\pi}} e^{-2t/3T_{1\rho}} \tag{37}$$

with the same constants as the model. The numerical and analytic models are compared in figure 2. As you can see, although the models match for the initial rise in spin polarization, they disagree on the rate of decay of that polarization in the phosphorus. The models are in agreement to within 10% for all times $\text{t} < T_{1\rho}$. And, for experiments done with very short contact times, less than about 3-5 ms in this case, there is little difference between

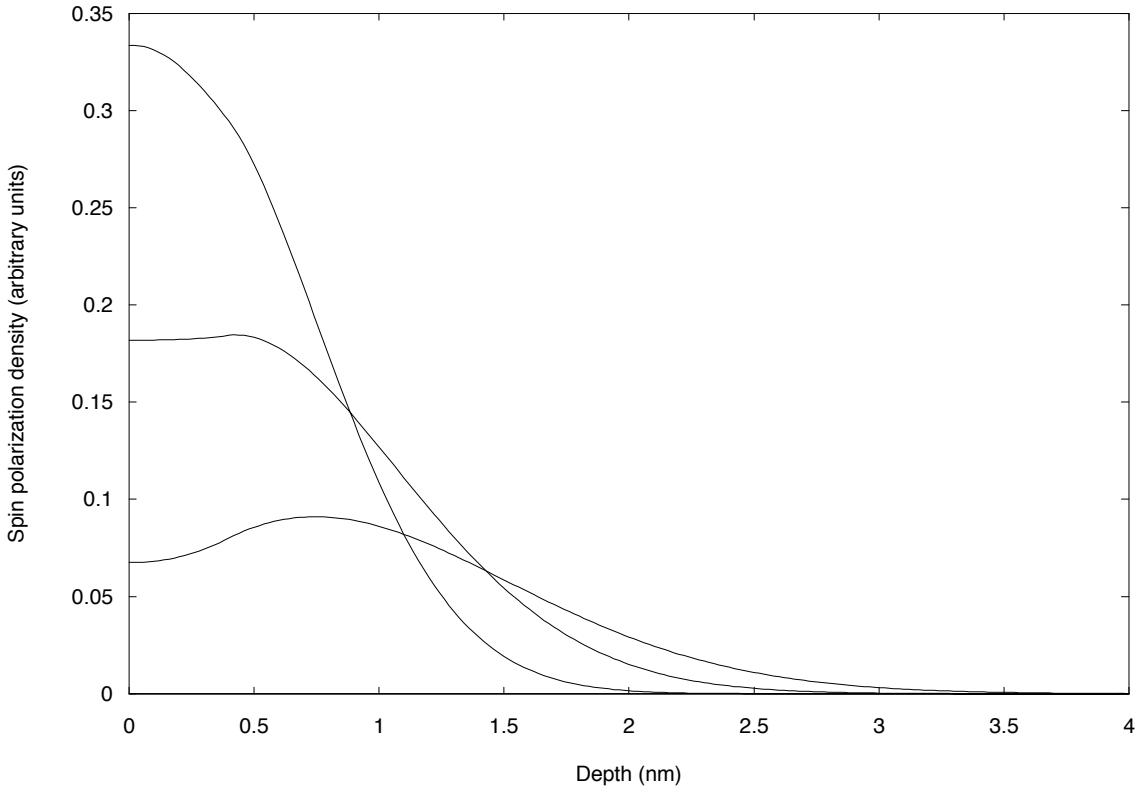

FIG. 1: Numerical model of spin polarization density, at 5, 10, and 25 ms (from top to bottom at x=0, respectively), normalized to initial spin polarization density.

the predicted curves. In this region, the analytic model is superior, as with only two free parameters and a simple functional form, it can be easily fit to data. Evaluating the numerical model with sufficient accuracy to produce reasonable graphs took a lot of computing time and power (several million excel cells were evaluated). Fitting the numerical model to data would involve tweaking several parameters by hand, and would lack a clear error estimate on those parameters. However, the results of spin diffusion involving contact times longer than $T_{1\rho}$ can be easily compared to qualitatively check this model. Finally, I tried fitting equation 37 to the numerical results, using Gnuplot to optimize the intensity and $T_{1\rho}$, using only the first 3 ms. The results for intensity did not significantly differ, but the $T_{1\rho}$ estimate was overestimated by 10%. A similar result was found using $T_{1\rho} = 16$ ms. This sets a reasonable best case limit on the accuracy of $T_{1\rho}$ measurements through these models.

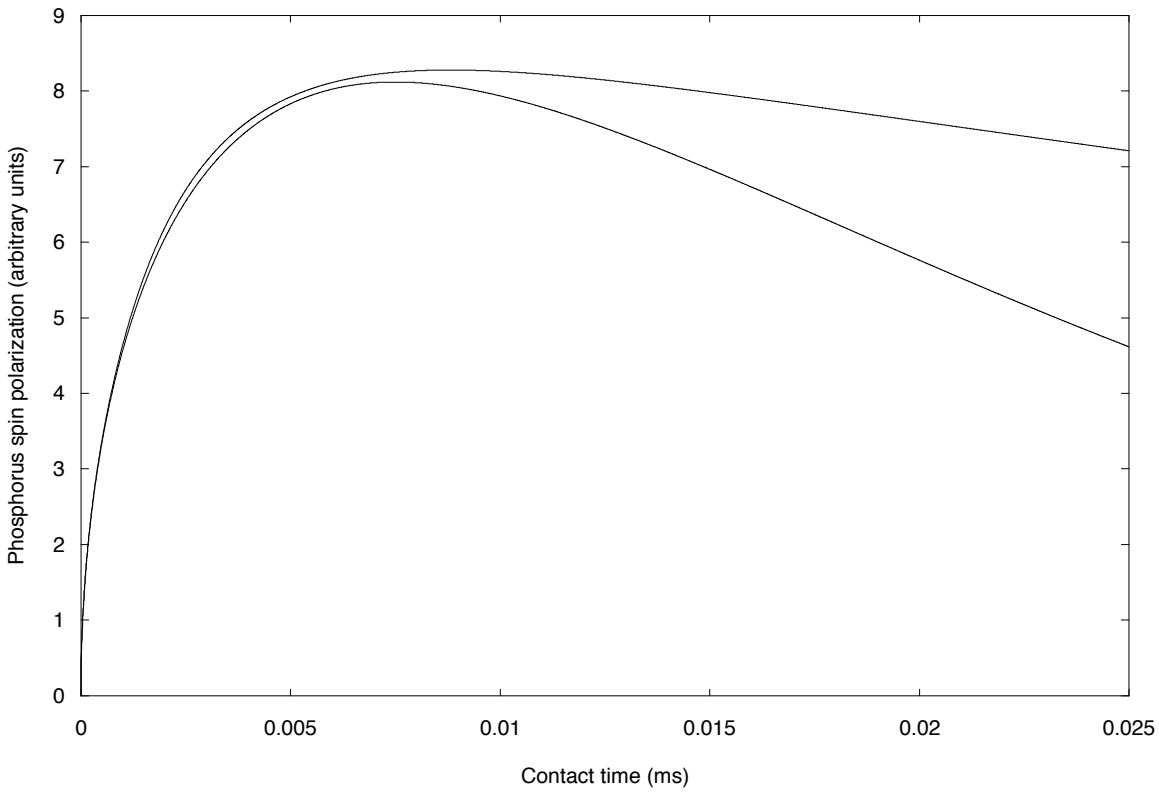

FIG. 2: Numerical model of the total phosphorus spin polarization (upper curve), compared to the prediction assuming a simple decaying source (lower curve).

B. Predictions of the diffusion models

The model from a decaying point source predicts the most experimentally observable behavior. Integrating equation 34 over the entire surface gives us the total phosphorus signal of the sample as

$$P(t) = A\rho(H)\epsilon\sqrt{\frac{4Dt}{\pi}}e^{-2t/3T_{1\rho}}. \tag{38}$$

Here, ρ(H) refers to the spin density of the hydrogen in TFMBB, D is the diffusion constant, A is the surface area of the sample, and $T_{1\rho}$ is the relaxation rate of the hydrogen spin reservoir, in spin lock. I have also included, for completeness, a surface efficiency parameter, $0 \leq \epsilon \leq 1$. A number of assumptions must be made to evaluate P. First, we assume that the surface is sufficiently smooth to allow the 1-d diffusion equation to hold – if this is not the case, we note that near a point (considering diffusion into a conical surface) or edge, the flow of spin into the phosphorus will be diminished. This geometric effect can be absorbed into ϵ, if need be. We also assume that there is no resistance to spin diffusion

across the organic-semiconductor interface while cross polarization occurs. In other words, we assume a polarized phosphorus (or hydrogen) nucleus at the surface is equally likely to transfer that polarization in either direction. As I cannot estimate either of these effects, and believe them to be minimal, we therefore assume, unless proven otherwise, that $\epsilon = 1$. We then assume that a thin layer, one molecule thick and completely coating the particles, of TFMBB is supplying the source of spin polarization during these experiments. We initially assumes that, as cross polarization is a dipole effect only occurring between very close molecules, any TFMBB not directly attached to the phosphorus will not interact with the semiconductor. But, as the measured $T_{1\rho}$ of the surface hydrogen is much shorter than the time for spin to diffuse even a few angstroms, this assumption can be easily relaxed. When I repeated my simulation with a hydrogen layer of 6 $\mathring{A}$, there was only a couple percent increase in the phosphorus spin polarization. However, if the organic molecule does not completely coat the surface of the InP grains, we could overestimate the expected spin polarization transfer. We also assume that the density of TFMBB is equal to that of the liquid form, where the specific gravity is 1.546 g/cm^3. This corresponds to a hydrogen density of $1.96 \cdot 10^{28} H/m^3$. With a Boltzman distribution of spin (as ΔE is small, I make the approximation $e^{\Delta E/k_B T} \simeq 1 + \Delta E/k_B T)$, this yields a spin density of

$$(1.96 \cdot 10^{28}) \frac{\frac{1}{2}(1) - \frac{1}{2}(1 + \Delta E/k_B T)}{2 + \Delta E/k_B T} \hbar/m^3 = 3.8 \cdot 10^{23} \hbar/m^3,$$

where ΔE is calculated from the energy of a photon required to excite the hydrogen resonance at 400 MHz. Finally, with no direct way to measure the diffusion constant, we shall also have to assume that the Lowe and Gade model, predicting $D \approx 3 \cdot 10^{-17}$ is correct.

This allows us to expect, for example, in a sample with 0.5 m^2 surface area at 22^{o}C, that

$$P(t) \approx 10^{15} \sqrt{t} e^{-2t/3T_{1\rho}} \hbar s^{-1/2}. \tag{39}$$

As many of our assumptions ignored effects that could decrease this flow rate (the TFMBB might not fully coat the particles, not all hydrogen might fully contribute, or the geometry might inhibit diffusion for example), this may be regarded as a tentative upper limit. However, the largest uncertainty is in the diffusion constant, D, which is only predicted to within a factor of about 2 or 3. If diffusion occurs within a range of 10^{14} to 10^{15} $\hbar$ $s^{-1/2}$, that is all that can be expected. The theory, however, does provide a valuable functional form that we can fit our diffusion data too. As we shall later see, this form is a very good fit to the data.

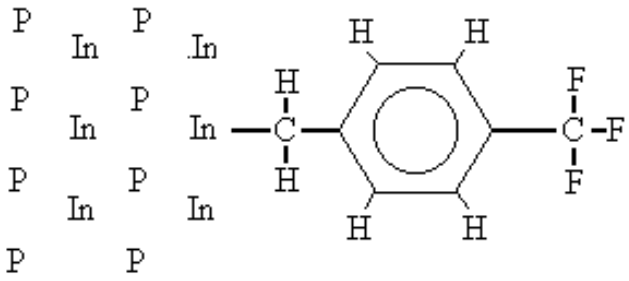

FIG. 3: The expected bonding of the 4-trifluoromethylbenzylbromine to the surface of an indium phosphide grain. The bromine atom is replaced by a carbon-indium bond.

IV. EXPERIMENTAL SETUP AND METHODS

A. Sample preparation

Bulk pieces of indium phosphide, a common semiconductor, were ordered from Aldrich, as was stock solution of 4-trifluoromethylbenzylbromine (TFMBB). The organic reagent was chosen because of it's small size, and the presence of a strongly interacting bromine atom. Spin diffusion had been previously observed, but not quantified, using these two chemicals [9].

Upon contact with indium phosphide, the bromine of the TFMBB reacts with the surface, as shown in figure 3. However, InP also reacts with oxygen and water in the air. To provide a clean surface for the TFMBB to bind to, the reagents must be prepared in an inert atmosphere.

I first diluted the stock solution of TFMBB with acetonitrile to form a 0.5 M solution. 2.00 ml of this solution was pipetted into a ground glass round bottomed flask. Approximately 0.25 g of InP chunks were measured into a small mortar and pestle. The flask, mortar and pestle were placed into a small glove bag, which was then sealed. To ensure that a clean, dry nitrogen atmosphere was in the bag, I inflated and deflated the bag three times with nitrogen. During each inflation, the flask was opened in the glove bag, and N_2 was sprayed into it to remove any residual air. In this N_2 atmosphere I ground up the InP, with mortar and pestle, and then dumped the resulting powder into the 0.5 M TFMBB solution. I then left the sealed flask in a water bath at 60^oC, for 2-3 hours. This allowed the TFMBB to bind to the surface of the InP; the reactive bromine tailing the organic molecule was expected to react with the indium and leave a carbon-indium bond. I was careful to keep

the temperature of the bath below the boiling point of TFMBB, given as 65-59^{o}C in the MSDS. The mixture was then taken out of the bath, and allowed to settle. To rinse the InP powder, the solution was decanted, and pure acetonitrile was added. I decanted the solution 4 to 5 times. After the final rinse, I let the remaining fluid evaporate. For the last sample, a centrifuge was used to help the smallest particles precipitate. The samples were divided, to give at least 100 mg of powder for NMR analysis, and up to 100 mg for surface area testing. Three samples were prepared, where the grinding time was 5,10 and 15 minutes. This was done to prepare a variety of surface areas, per unit mass, for the experiment. The NMR samples for the first, second and third powder samples are, respectively, 0.1207 g, 0.1005 g, and 0.1857 g.

B. Surface area measurements

Initially, I was working with a Micrometrics ASAP 2000 surface area measuring machine. This device takes a powdered sample, and attempts to measure the surface area by analyzing the volume of adsorbed gas that sticks to the particles at different pressures. Essentially, it consists of feeds to analysis gasses, various pumps, a cold trap, and temperature and pressure sensors. A sample is loaded into a sample tube, and then evacuated. To remove any residual surface contaminants from the air, the sample is then cooked at 350^{o}C, under vacuum, for several hours. It is then pumped to a full atmosphere of the analysis gas, usually nitrogen, and re-evacuated. Once the pressure has dropped to the pumping limits, an analysis run can be started. The sample tube is suspended over a bath of liquid nitrogen. The tube is partially surrounded by a seemingly useless plastic tube, and a styrofoam circle is placed at the top to slow down the evaporation of the N_2 bath. During analysis, the sample is moved into the N_2 dewar, and set amounts of analysis gas are repeatedly pumped onto the sample, the pressure is measured, and the gas evacuated. This machine is very, very, finicky, and in order to even come close to repeatable results, this full procedure needed to be repeated exactly before every run. The analysis results are a measurement of the BET and Langmuir surface areas. There was little difference between these two results, however, as the BET results quoted lower error, they seemed preferred. When I report surface areas, they are the BET measurements.

While I was working with the Micrometrics machine, it was in the process of a long,

excruciating breakdown. Thus, even after a valiant struggle, I was not able to get believable results from it. Instead, I was forced to find an alternative.

To complete my surface area testing, a Mastersizer 2000 was used. This is a simpler, and more reliable measurement, and can be done much more quickly than tests on the Micrometrics equipment. The test is non-destructive, and only takes 20 s. The InP powder is suspended in water. In this suspension, the particles tended to clump up, but through vigorous stirring and ultrasonic vibration this problem was minimized. Blue light is shone through the sample, and by measuring the scattering angle and intensity, one can estimate the particle size and surface area distribution. Only preliminary measurements have been done with this instrument.

C. NMR setup and pulse programs

I used a 9.4 Tesla Varian/Oxford NMR spectrometer, with hydrogen resonance at 400 MHz, for my experiments. About 100 mg of prepared sample was packed into a sample rotor, and placed into a double resonance probe. The system was tuned to deliver RF pulses at the hydrogen (399.749 MHz) and phosphorus (161.797 MHz) resonant frequencies. Hartmann-Hahn cross-polarization conditions were used, as outlined in the introduction, to allow spin to move back and forth between hydrogen and phosphorus. To perform the range of experiments I wished to study, I had to modify the Varian xpolar1 pulse program. This program allows cross-polarization to be directly followed by measurement. I created the xpbakup program to include a delay, d3, between cross polarization and acquisition. During this delay, the phosphorus spin polarization is stored along the external magnetic field, and accessed, via a pair of $\pi/2$ pulses. The xp2 program adds a second cross-polarization phase after this delay, to allow spin polarization to be returned to the hydrogen nuclei. The pulse programs are summarized in figure 4.

In xpolar1, a $\pi/2$ pulse is immediately followed by a spin locked cross polarization pulse, with a phase difference of 90^o, and an acquisition period either in phase, or 180^o out of phase with the spin lock pulse. Repetitions of an experiment, of which there were typically several thousand, cycle through four different phase cycles – with the phase of the initial pulse changing, along with the phase of the acquisition period. These changes average out any signal that would otherwise grow into the phosphorus or hydrogen as a result of T_1 relaxation.

This ensures that the only signal reported is that which has diffused into the phosphorus from the hydrogen. The xpbakup and xp2 programs had significantly more complex phase patterns, but their phase cycles achieved the same effect. These phase cycles are mainly used to average out distortions in data due to T_1 relaxation during the experiment.

V. RESULTS

A. Optimizing the cross-polarization signal

The first experiments I performed were to check that spin polarization did in fact diffuse across the InP-TFMBB boundary. These experiments were done using the simple, and prewritten, pulse program xpolar1. In the process I optimized the cross-polarized signal with regard to the program parameters.

First, several of the parameters were assigned by the program. The phosphorus frequency was set to 161.797 MHz, with an offset of -24536.4 Hz. The hydrogen frequency was 399.749 KHz with a -879.2 Hz offset. To see the phosphorus peak, which initially had an unknown chemical shift, a sweep width of 100 KHz was chosen. The peak proved to be quite broad, and this width was retained as a good scale for it's resolution. 1024 points were taken, corresponding to 512 real and 512 imaginary parts, giving a resolution of about 200 Hz. For most experiments tens of thousands of repetitions were made, usually ranging from 20 000 to 100 000, depending on data quality and time constraints.

The delay time between repetitions, d1 in figure 4, needed to be chosen as much greater than the T_2 of the phosphorus, and the T_1 of the hydrogen. In effect, there had to be enough of a delay between repetitions of the pulse sequence to allow the hydrogen to return to an equilibrium state. The other parameters were calibrated using a reference sample. As the $\pi/2$ pulse width should not vary significantly across different molecules, phosphoserine was used to determine that a hydrogen $\pi/2$ pulse should be about 4.4 μs. The contact time was arbitrarially set to 2 ms. After testing a couple delay times, I chose to set it to 0.5 s. There was no visible difference between results at 1.0 s, and 0.5 s after 100 000 repetitions. Below 0.5 s lurked the hydrogen T_1, which remains unknown. Unless otherwise noted, this delay period was constant through all of my experiments.

I then moved on to optimize the contact time. With d1 fixed at 0.5 s, I ran the xpolar1

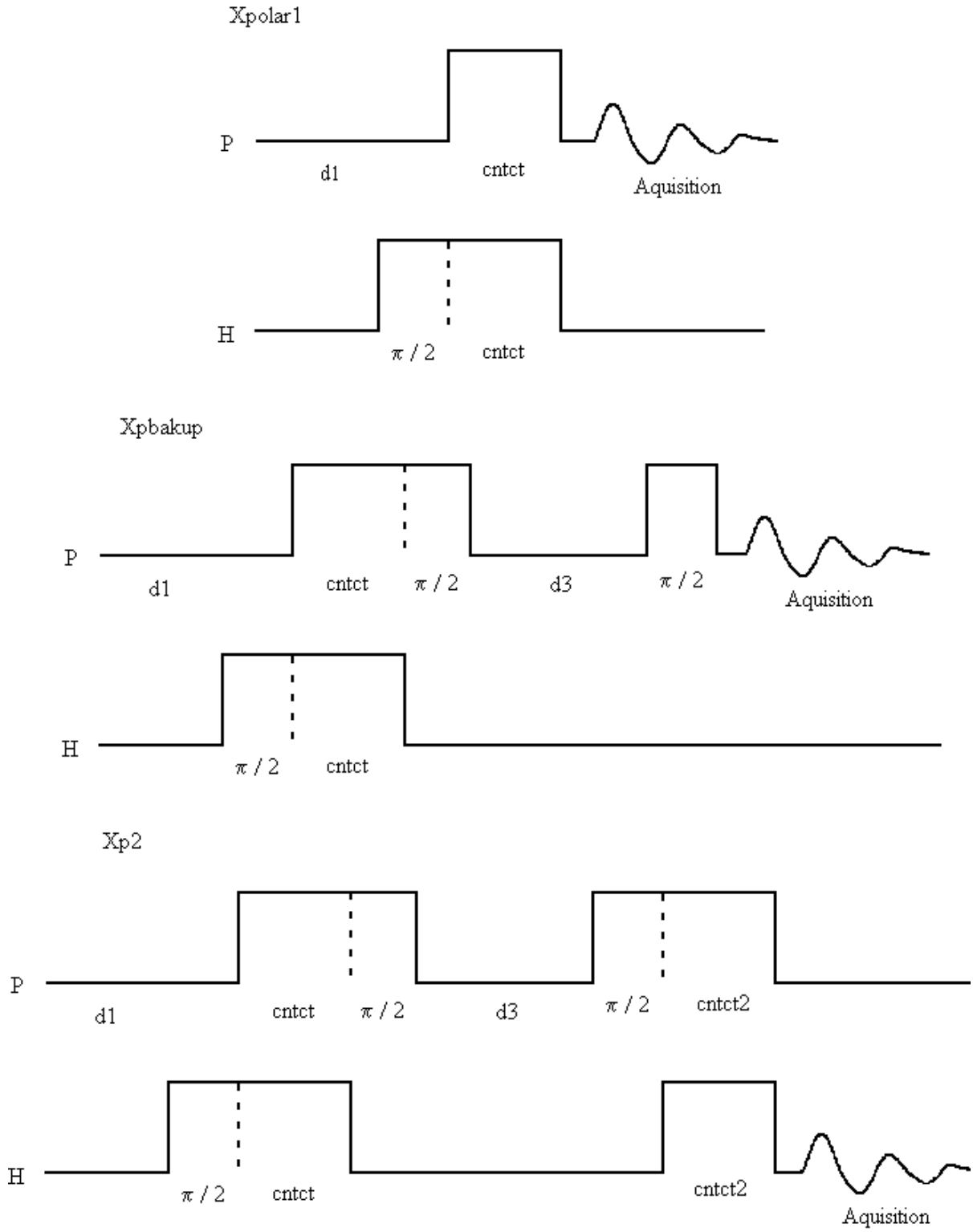

FIG. 4: The pulse programs used during my experiments. Xpolar1, provided by Varian, allows simple cross-polarization. Xpbakup incorporates a pair of $\pi/2$ pulses to store spin in the phosphorus before acquisition. Xp2 has a second cross-polarization phase to allow spin to diffuse back into the hydrogen.

pulse sequence with 50 000 repetitions from 3 to 27 ms, in 3 ms steps, and with 100 000 repetitions at a few smaller times. The intensity appeared to be relatively constant between 6 and 27 ms, while dropping off at lower times. Visually comparing the height of the peaks, I chose 18 ms as the optimal contact time. Upon later analysis, this proved to be false, as the phosphorus peak narrows at larger times, leading to a decline in signal intensity after about 10 ms. The difference was quite small, as the slow decline of the model in figure 2 suggest.

The last parameter to be optimized was the phosphorus $\pi/2$ pulse width. With 50 000 repetitions, I checked times from 0 to 18 μs, in 1.5 μs intervals. At this point, I had not yet developed my analysis procedures, and did not have access to reliable software. I estimated the $\pi/2$ width by eye. As I was not able to distinguish any differences from the 4.4 μs value suggested from phosphoserine, I continued to use that width. After fitting a Gaussian shape to the processed data (as described in the following section), the phosphorus intensity is plotted in figure 5. Only spin polarization in the x-y plane should diffuse under cross-polarization, and so the signal should vary sinusoidally as the polarization vector is rotated. Fitting the function $\sin(\omega t) + c$ to the results gives a period of 18.7 μs. There is a slight offset, as c is not 0, corresponding to about 5% of the maximum signal. This may be due to phosposerine contamination, which will be discussed later. Using this analysis, the $\pi/2$ width is 4.7 μs. As with the contact time, the final analysis of my data shows my initial optimization was not perfect, although it was adequate.

The sinusoidal variation in phosphorus signal, as the hydrogen spin polarization was changed, is evidence that the observed signal must have originally come from the hydrogen. This was my first evidence that I could measurably diffuse spin polarization across my interface.

In these optimization experiments, magic angle spinning was used, from 3000 to 5000 Hz. However, once a strong signal had been teased out of the sample, it became apparent that spinning did not narrow the peak. Indeed, there are theoretical reasons why magic angle spinning might inhibit spin diffusion. The spin exchange term in the Hamiltonian 4 depends upon the term $(1 - 3\cos^2(\theta_{ij}))$, which is exactly 0 at the angle chosen to eliminate dipolar broadening under magic angle spinning. Although I was never able to test whether spinning decreased the diffusion rate, as it wasn't obviously doing any good I discontinued use of magic angle spinning for all experiments other than the initial optimization.

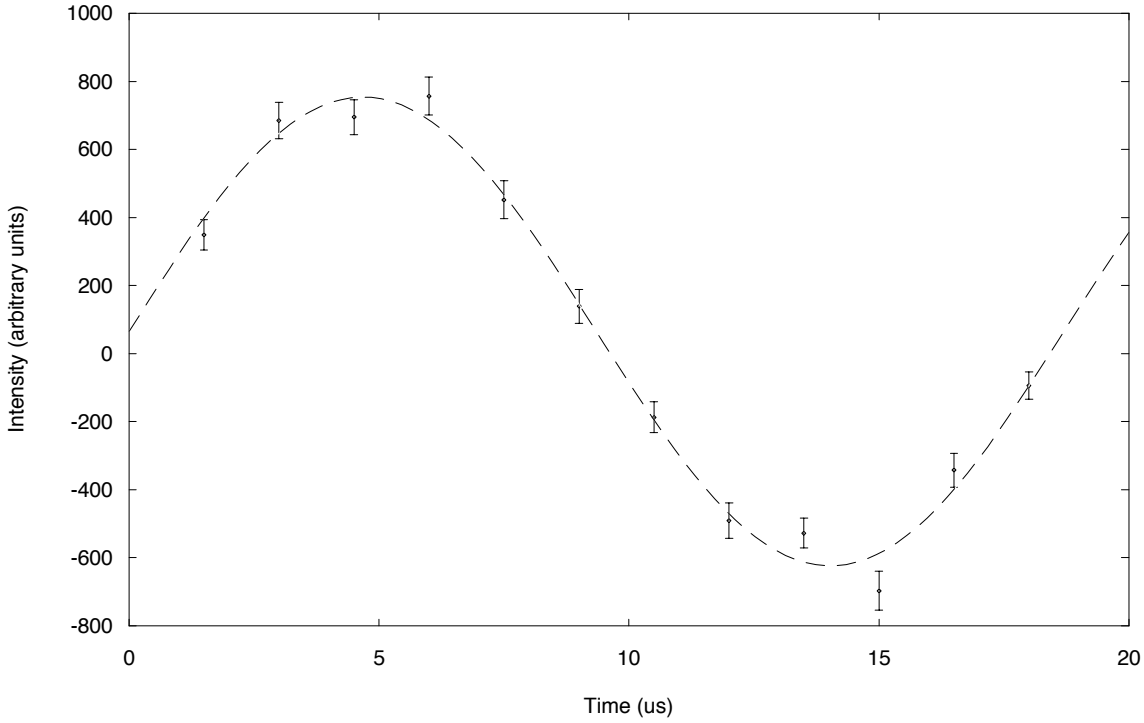

FIG. 5: Data used to optimize the hydrogen pi/2 pulse width, with best fit sine curve.

B. Calibration and T_1 measurement

I wanted to determine the rate of spin diffusion, in an absolute value of the number of quanta of spin polarization crossing an organic-semiconductor boundary, as a function of contact time. Since the measurements were done using NMR spectroscopy, some calibration was necessary to determine how to translate the signal intensity into the number of polarized nuclei.

To begin with, I needed a consistent way to measure the intensity of an NMR peak. Most of these experiments involve very small effects, and require thousands of scans to detect a signal from the few phosphorus which have gained polarization from the TFMBB. During early experiments, a smaller peak began to appear near the semiconductor phosphorus signal. It is a rather small, and often ephemeral peak, with a frequency shift above that of the InP phosphorus (and thus appearing to the left of the InP peak). The signal was likely identified to be residual phosphoserine, left over from the previous use of my sample tube. It has the same frequency shift as phosphoserine (as a quick scan of an available phosphoserine sample showed) , although the signal persisted after the tube was cleaned for the 2nd and 3rd InP

samples. However, during experiments with varying cross-polarization times, this peak did not change size, while the main peak varied by over an order of magnitude. This is a clear evidence that the little peak is not related to the spin diffusion signal of interest.

However, the nearby phosphoserine contamination meant that I could not effectively find the intensity of the InP phosphorus peak by simply integrating the signal intensity over some frequency range. The width of the InP peak was also variable, as the chemical shift of the surface atomic layer phosphorus is not the same as the chemical shift of phosphorus further inside the particle. This disqualified using the maximum height as a marker. Instead, I chose to fit to the Gaussian function,

$$f(x) = 1000(\frac{I}{\sqrt{2\pi\sigma^2}}e^{-(x-\mu)^2/2\sigma^2} + C). \tag{40}$$

Here, I is the intensity I will be reporting in the future, C is a baseline correction, and the factor of 1000 is included to make I into a reasonably small number. The variable x is related to the frequency shift: the entire data set covers up to a 100 KHz chemical shift from the phosphorus resonance at 161.7725 MHz. Usually, either 256 or 512 data points cover this range. I converted the Varian NMR data files into a usable form using XNMR, a program that was available in my lab for analyzing Varian's data format. I used Gnuplot v. 3.71 to do my fits.

To test the repeatability of both the raw data, and the method of characterizing it, I repeated a simple cross-polarization experiment six times. I used the xpbakup program using 4.4 ms $\pi/2$ pulses, 18 ms of contact time, and a 100 ms delay before acquisition. These parameters were chosen to give me a large signal. 20000 scans were taken in each repetition. An example of the raw data, typical of many of the experiments I performed, is provided in figure 6, along with its Gaussian fit. The results of these six trials – the fit values of μ, σ,I, and C – are provided in table I, along with the relative uncertainties in all the parameters. The final row summarizes the sample error of the six measurements. We expect the signal to noise ratio to increase as $\sqrt{I}$. So, to get the uncertainty of further fits I used these relative uncertainties, weighted by the ratio $\sqrt{223.6/I}$, or the fit error, whichever was greater.

Before an accurate bulk phosphorus signal could be take, I had to measure the phosphorus T_1. Based on a colleague's research, I expected the T_1 to be about 300 s [10]. To find T_1, I measured the phosphorus signal after a 4.4 ms pulse placed the phosphorus magnetization

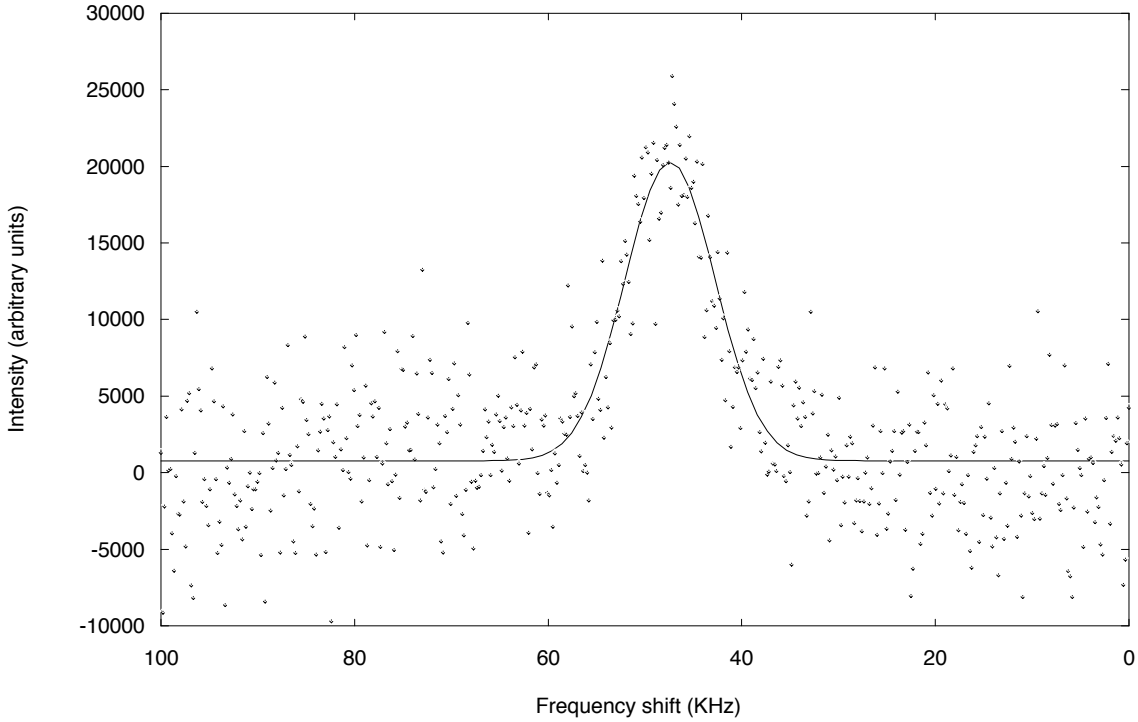

FIG. 6: An example of a gaussian fit to cross-polarization data, used to determine the accuracy of the fit when comparing data sets.

into the xy plane. I took four repetitions at each of a 5, 50, 200, 400, 800 and 1600 second delay between experiments. Fitting an exponential to the data gives the T_1 as 287 $\pm$ 47 s. This was consistent with the expected value, and justifies the assumption that the phosphorus signal is constant on the time scale of my cross-polarization and diffusion experiments (from a few ms of cross polarization to, at most, 20 s of further spin diffusion). The data is presented in figure 7.

I am now able to calibrate the scale of the phosphorus peak. I set the temperature controller to maintain 22^oC in the sample. A time delay of about 10 times the phosphorus T1 should provide me with a fully regenerated phosphorus magnetization for every sweep. Choosing an hour delay between each of 48 repetitions gave me a very good signal. This gave me the peak shown in figure 8. The best fit Gaussian has $I = 928.5 \pm 5.0$, $\mu = 48.56 \pm 0.02$ KHz, and $\sigma = 2.72 \pm 0.02$ KHz. But, given the earlier test of the accuracy of this fit, these errors are too small. In particular, we expect about a 1% error in I. The intensity, per scan, is then 19.34 ± 0.2.

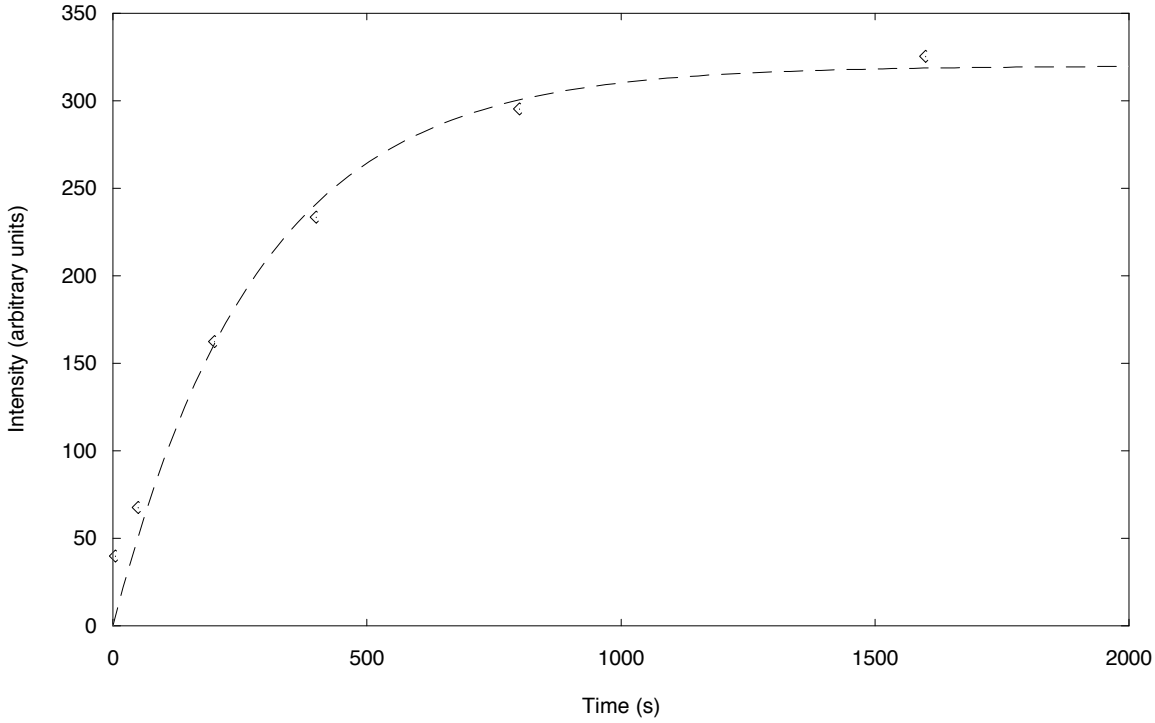

FIG. 7: Data from the measurement of the phosphorus T1, with an exponential best fit.

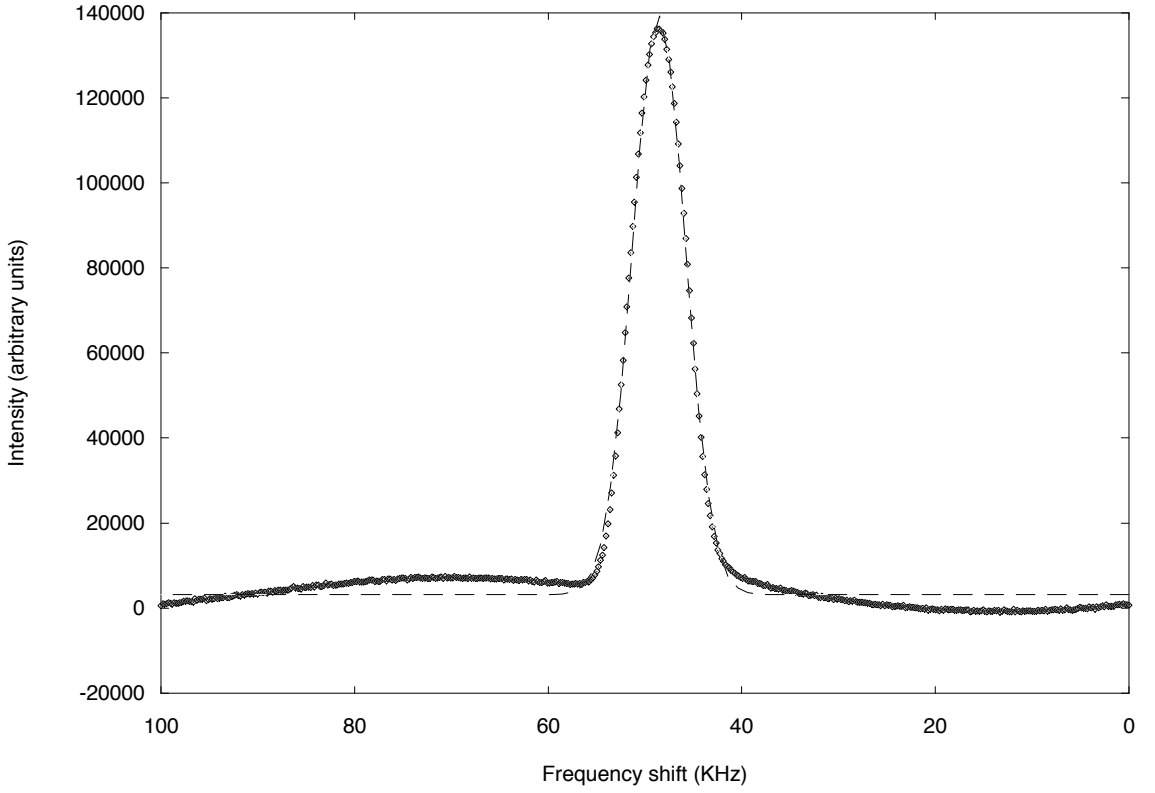

FIG. 8: Calibration data for a bulk phosphorus signal, with gaussian fit.

Experiment	I	σ	μ	C
1	221.1	4.55	47.66	1.06
2	226.8	4.45	47.85	0.37
3	228.0	4.65	47.46	0.78
4	227.0	4.18	47.75	0.84
5	217.8	4.67	47.66	0.54
6	220.7	4.59	47.66	1.73
mean value	223.6	4.52	47.68	0.89
fit error	9.2	0.20	0.20	0.19
standard error	4.2	0.18	0.13	0.48
relative uncertainty	2%	4%	0.25%	50%

TABLE I: Comparison of gaussian fit parameters to 6 identically conducted experiments. The fit errors represent the size of the uncertainty provided by the fitting routine output. The standard error is the square root of the variance of the six measurements, and the relative uncertainty is the ratio of the standard error to the mean value of a parameter.

Note that the baseline in figure 8 is not flat. In order to get a consistent measure of the intensity, I was not able to clean up the data by cutting the first few points off the free induction decay. Distortions in the first 2 or 3 data points of this decay, when fourier transformed, leads to experimental artifacts in the baseline. In later experiments, for example, the phosphorus peak often sat in a shallow valley. In experiments where I did not need an absolute measure of the spin polarization I made the appropriate cuts to the free induction decays, to flatten out the baseline.

To calculate the expected number of polarized phosphorus nuclei, note that phosphorus has a spin 1/2 nucleus with a resonant frequency of 162 MHz in the spectrometer used. Since ΔE=$\hbar$f, then assuming that $e^{\Delta E/k_BT} \simeq 1 - \Delta E/k_BT$, the expected spin polarization is

$$\frac{\frac{1}{2}(1) - \frac{1}{2}(1 - \Delta E/k_BT)}{2 - \Delta E/k_BT}\hbar/\text{atom} = 6.60 \cdot 10^{-6}\hbar/\text{atom}.$$

With a molecular mass of 145.6 g, the 0.1207 g sample used for this calibration contains $4.98 \cdot 10^{20}$ phosphorus atoms. This gives an expected magnetization of $2.99 \cdot 10^{15}\hbar$. Thus,

one unit of I, per scan, is equivalent to $1.55 \pm 0.02 \cdot 10^{14}\hbar$.

C. Surface area measurements

1. Micrometrics ASAP 2000

Gentle reader, I have yet to inflict upon you the true horrors of surface area measurement. Beware. I prepared 3 coated indium phosphide powders, with different surface areas. In order to check my theoretical predictions, I need to know the surface area per unit mass of each sample, accurate to at least an order of magnitude estimation. Further, to make valid comparisons between my samples, I need a surface area test which can effectively discriminate between them. Based on cross polarization results to be discussed in the following section, this requires precision better than 50%.

This sounds simple, as surely some experiment can distinguish 1 m^2 from 10 m^2. With nice, macroscopic, and flat surfaces, this is easy. However, with little bumpy grains of dust the problem is not trivial. I had sole access to a Micrometrics ASAP 2000 for six weeks. Unfortunately, there was no expert of the machine available, only another relatively new user. Over time, I performed many surface area tests, slowly figuring out the best way to get results. Initially, I discovered the machine can easily give wildly varying results, including such unphysical things as negative pressures and negative surface area. Repeatability was only possible if, in addition to strict attention to seemingly irrelevant details (the initial level of liquid nitrogen in the dewers, the presence of a styrofoam heat shield atop the sample tube, the delay between cooking the sample and analysis...), a great deal of luck was had.

Concentrating on analyzing the first InP sample, I tried a number of things to increase the precision of the instrument. My results are listed, in chronological order, in figure 9. This figure does not include runs which failed to collect any data, or which produced blatantly unphysical results. Early runs found surface area by fitting a line to 5 adsorption measurements at different pressures; I eventually raised this to 40 points hoping that better statistics would help. They did not. I tried obsessively checking irrelevant details, to little effect. I tried substituting argon for the analysis gas, which was initially nitrogen. This should have lead to better results, but as experiments numbered 5 and 6 show, it did not. I have presented one negative surface area measurement with the argon, although there were

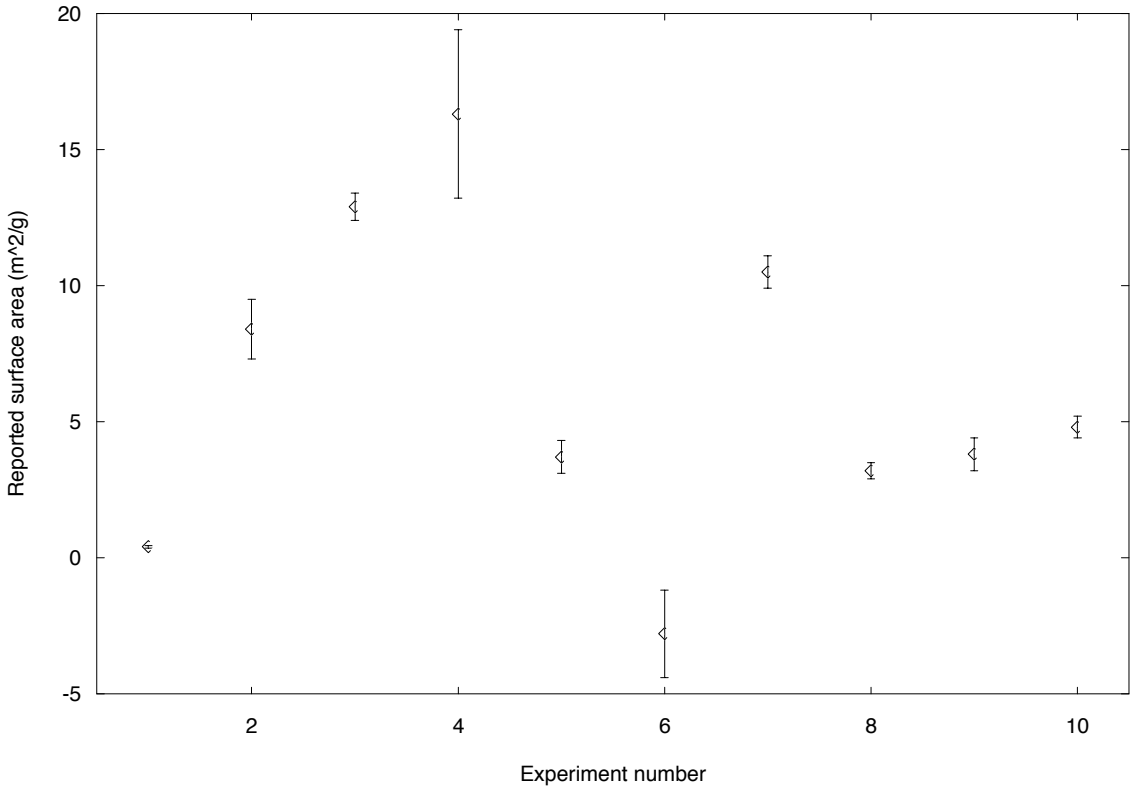

FIG. 9: Micrometrics surface area measurements on sample 1, labelled chronologically. Sample mass = 0.0307 g.

more.

After switching back to nitrogen, I had time to do a few more tests before a total breakdown of the equipment. During the earliest runs, I had encountered a curious error message of power failure. The first two, well separated, reported failures caused me some worry, but nothing beyond questioning the stability of the power source, and asking about possible power cuts/fluctuations in the chemistry building. However, over time the frequency of equipment power failure increased. During mid-February, while I was playing with argon analysis, I discovered that power failure was happening most nights, and was beginning to get used to yet another quirk of the machine. Unfortunately, failures during analysis were never reported, just power failures while the equipment was idle. This lead me to question the validity of the results, and careful scrutiny of the raw data showed that there were disturbing spikes in the pressure-adsorption curves.

Before I could get much further, I actually managed to catch a power failure occur while I was refilling the machine's liquid nitrogen dewers. The power flickered on and off for several

minutes, before settling down. Pumps hummed on and off, along with LED's, and valves closed down to prevent damage to sensitive equipment. After a few days of hesitant stability, the power failures returned, with the equipment starting up every few seconds to be almost instantly shut down by some problem. After several hours of tinkering with the innards of the machine, Jerry (the other, slightly more experienced user) and I were able to trace the problem, most likely, to either a transformer or a diffusion pump. However, at this time, I still do not know exactly what caused the surface area equipment to break down.

A simple average of the measurements of figure 9 suggests sample 1 has a surface area of about 6.4 m^2/g. With a 0.0307 g sample, this corresponds to 0.2 m^2. Unfortunately, I managed to perform a test on an empty sample tube, which managed to record a surface area of 0.3 m^2. It seems, in other words, that the measurement cannot even see the surface of the powder I have supplied. The one piece of information I can take from struggling with this apparatus is a best-guess upper limit of the surface area. Based on my results here, a surface area greater than 10 m^2/g would be surprising. This is a most unsatisfactory result, as 10 m^2/g is a huge surface area, and should be a surprising result anyway.

2. Mastersizer 2000

After the failure of the Micrometers instrument, both in its ability to collect informative data, and in its ability to work at all, I turned to other means to estimate the surface area of my InP powders. At short notice, and with some cajoling, a lab college was able to make some preliminary measurements on my first and second samples with a Mastersizer 2000. The first measurement was done on the 0.0307 g sample I was working with on my surface area measurements. He had problems with the analysis, as the particle density when suspended in water was below the machine's stated threshold, although he was able to get consistent results four times in a row. The best measurement of the surface area of sample 1 is 0.305 m^2/g. An error estimate on this figure is currently unavailable. The distribution of particle size has three different peaks, suggesting that certain radius particles went undetected. With the second sample, approximately 0.1 g was available to test, which produced a suspension above the threshold density. The one measurement performed gave a single peak in the particle size distribution, centered at 25 μm, and gave a surface area of 1.84 m^2/g.

The second sample should have a higher surface area than the first sample. Thus, I find the results of these tests to be, so far, unsatisfying. They have the advantage, over the Micrometrics tests, of actually detecting something, and supply a believable distribution of particles sizes. For my subsequent analysis, I shall assume that the measurement of 0.3 m^2/g for sample 1 is correct, or that at least the surface area is of that order. In order to confirm these measurements, I would like to spend some time acquainting myself further with the test equipment. I would also like to observe the particle size distribution directly, under a microscope. Both these options are open to future study, although I have not yet had time to start either of them.

D. Comparative cross-polarization experiments

Spin polarization diffusion between the hydrogen surface layer and the phosphorus nuclei has now been observed and optimized. The next thing to do is to check that the experimental results conform to the expected behavior. Recall that the model I developed suggests that, for short contact times, the phosphorus spin polarization should grow as

$$P(t) = I\sqrt{t}e^{-2t/3T_1}, \tag{41}$$

where all the parameters have been measured or can be calculated. The intensity $I = A\rho(H)\epsilon\frac{4D}{\pi}$, with constants as previously defined. During the optimization experiments, it was seen that the initial growth of phosphorus spin polarization occurred in the first 3 ms of contact time. This provides an easy means to confirm the model.

For sample 1, with a surface area of 0.3 m^2/g, a mass of 0.1207 g, at a stable room temperature of 22^{o}C, the phosphorus spin polarization is expected to follow

$$P(t) = 7.1 \cdot 10^{13}\sqrt{t}e^{-2t/3T_1}\hbar s^{-1/2}. \tag{42}$$

Using the pulse program xpbakup, with optimized parameters, I investigated the cross-polarization range from 0.2 to 4 ms. I used a 0.5 s delay between cross-polarization and acquisition. I found that such a delay sharpened the phosphorus peak, as it allowed much of the phosphorus spin polarization to diffuse into the interior of the InP grains. As I later show, there is noticeable chemical shift between the surface phosphorus nuclei, and those inside the grains. 64 000 repetitions were taken at each point. The results are shown in

figure 10 with a best fit of I = 3.7 ± 0.2· 10^{13} $\hbar$ $s^{-1/2}$, and T_1 = 7.3 ± 1.4 ms. This is in remarkable agreement with the model, considering the many assumptions built into it, and the large uncertainty in D.

As it plateaus, the phosphorus has acquired a spin polarization of almost $1.7{\cdot}10^{12}\hbar$. The total initial spin polarization in the hydrogen surface layer can be estimated as

$$P(H) = dA\rho \simeq (4 \cdot 10^{-10}m)(0.3m^2/g \cdot 0.1207g)(3.8 \cdot 10^{23}\hbar/m^3) = 5.5 \cdot 10^{12}\hbar. \qquad (43)$$

Here d = 4 $\mathring{A}$ is an estimated width of the hydrogen source layer. It is the same width I used in my numerical simulation. A is the surface area of the sample, and ρ is the hydrogen spin polarization density, as previously calculated. This calculation suggests that about 30% of the hydrogen spin polarization can enter the phosphorus. This compares well to the observation, in my numerical model, that about a third of the hydrogen polarization was eventually transferred into the phosphorus. It also shows that spin diffusion can transfer significant amounts of spin polarization across the organic-semiconductor interface.

For sample 1, the hydrogen T_1 is found to be only about 7 ms, and the spin polarization is already beginning to plateau with the measurement at 4 ms. From numerical simulations, we know that equation 41 is only suitable for the steep, initial climb of phosphorus spin polarization. Therefore, to stay within a suitable cross-polarization time, for further experiments, I decided to reduce the maximum contact times used to calculate I and T_1 to only 2 ms.

With this modification, the same experiment was done with samples 2 and 3. The results, with fits, are shown in figures 11 and 12, respectively. All three experiments are consistent, and are summarized in table II. The value of $T_{1\rho}$ is, when weighted by all three measurements, 7.8 ± .4 ms. Although the surface areas of the different samples are not known, by taking a ratio of the intensities per gram of various samples, I can predict the differences in surface areas. It is comforting that both sample 2 and sample 3 show larger signals than sample 1, however the signal from sample 2 is not as large as I would expect. That sample was subject to the most grinding, and was carefully washed, using a centrifuge to keep the smallest particles. It should have a significantly higher intensity.

This consideration aside, these three measurements show that the model I proposed can explain these results effectively and consistently. The spin polarization signal in the phosphorus does, as expected, have some positive dependance on the surface area. From

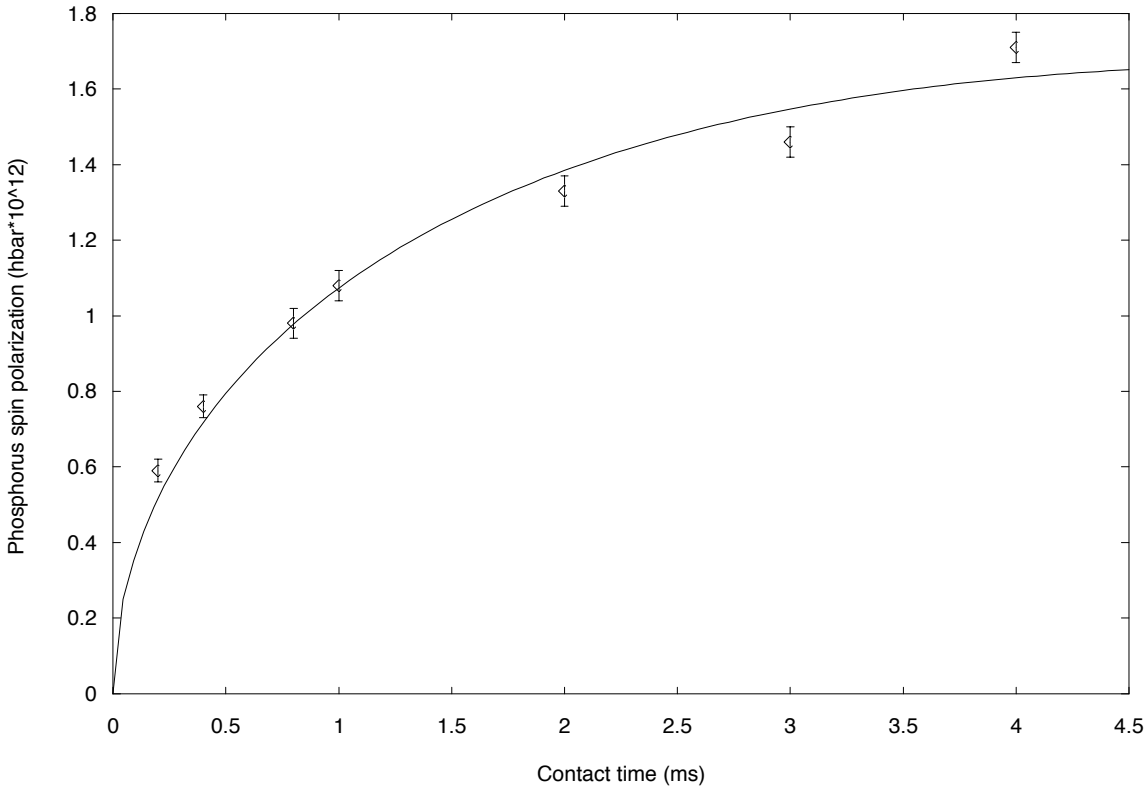

FIG. 10: Observed phosphorus spin polarization in sample 1, versus contact time.

Sample number	Mass (g)	Fit intensity (10^{12} $\hbar$ $s^{-1/2}$)	Fit $T_{1\rho}$ (ms)	Relative surface area (/g)
1	0.1207	37 ± 2	7.3 ± 1.4	1.00
2	0.1005	48 ± 1	8.3 ± 1.9	1.56
3	0.1857	61 ± 1	6.5 ± 0.9	1.06

TABLE II: Summary of cross-polarization experiments on three different samples. The relative surface area is calculated by comparing the fit intensity, per gram, of a sample to that of sample 1.

this model I can confirm the rough order of the diffusion constant as calculated from either Lowe and Gade, or Redfield and Yu.

E. Low temperature experiments

One parameter that can easily be checked in equation 38 is the dependance on the surface hydrogen spin density, $\rho(H)$. This should vary under changes in temperature. I

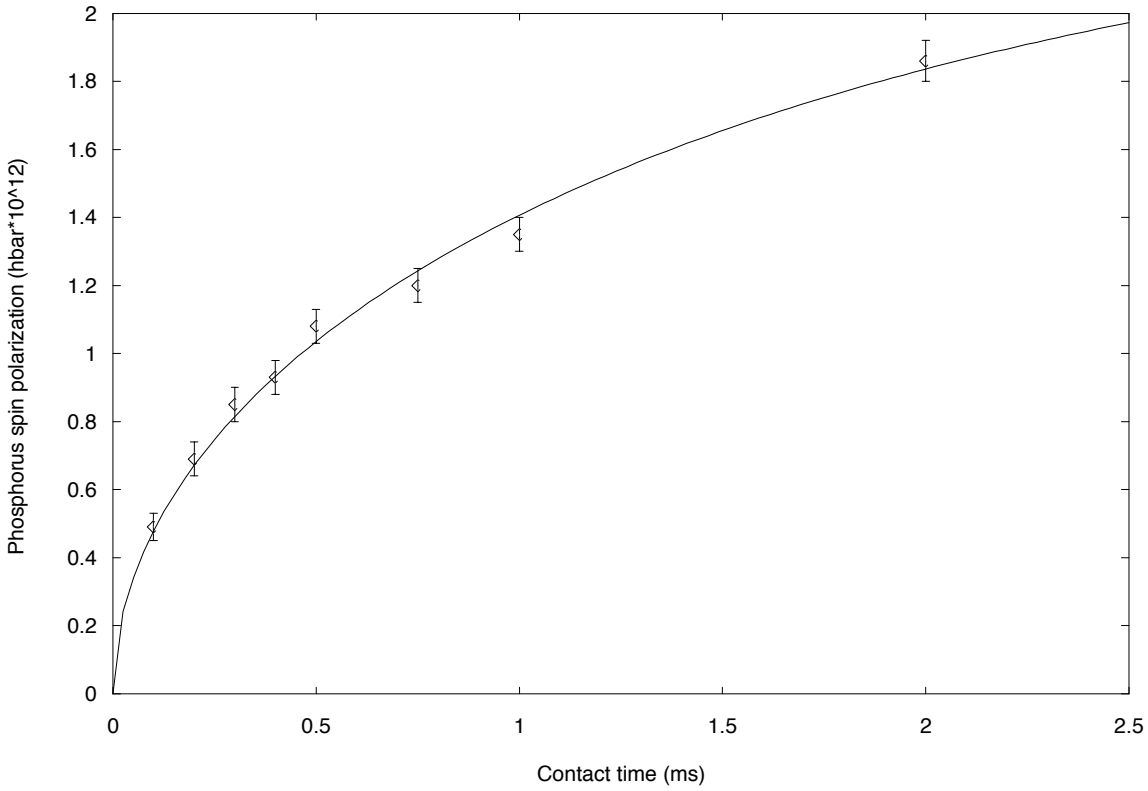

FIG. 11: Observed phosphorus spin polarization in sample 2, versus contact time.

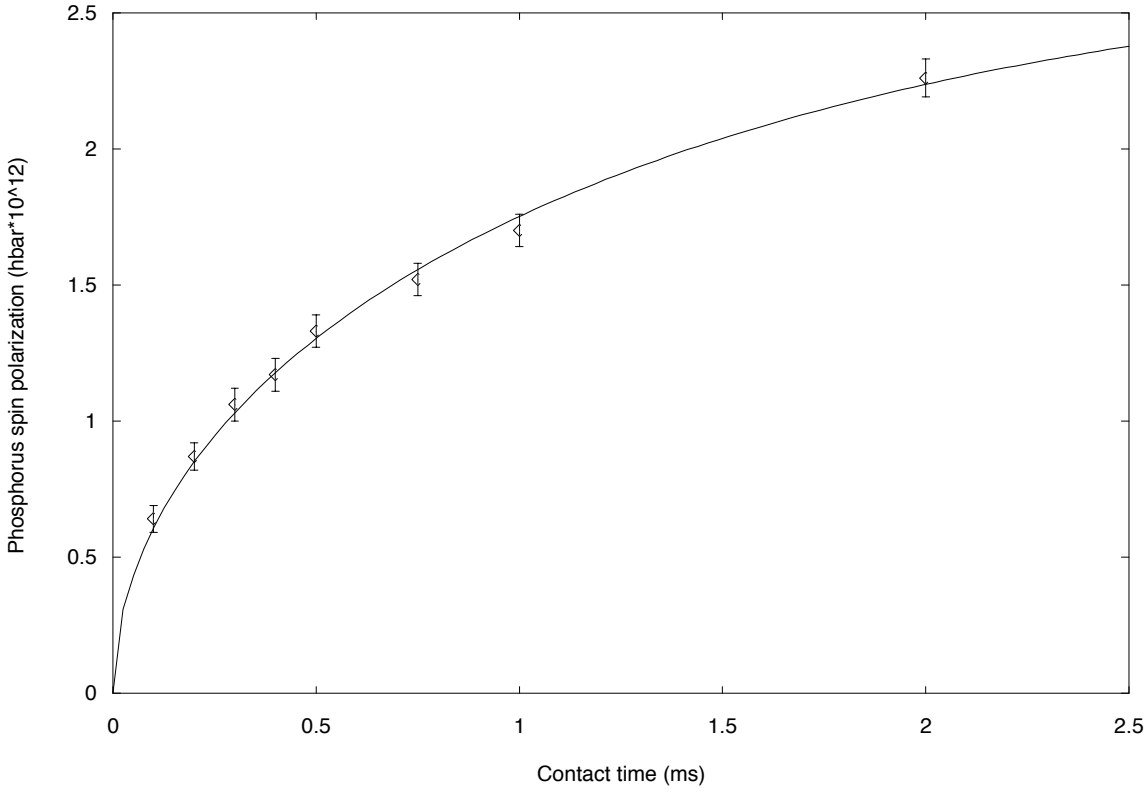

FIG. 12: Observed phosphorus spin polarization in sample 3, versus contact time.

was able to cool the sample down to -45^{o}C, and perform an experiment on sample 1 to test this dependance. Since we are dealing with extremely small spin polarizations, the spin polarization density should be inversely proportional to temperature. This predicts that at this low temperature the signal intensity should by increased by a factor of (273+22)/(273-45) = 1.29. Although I used an identical procedure as in the previous section, I had to check to make sure that the probe sensitivity was unaffected by the temperature change. This is a concern, as the electrical properties of the rf coil are temperature dependant. To check how the coil would give, and receive, rf fields, I performed one of the calibration routines already discussed. With the same settings I used to generate figure 5, discussed in the optimization section, I checked the response of the cross polarization signal as the $\pi/2$ pulse was varied between 0 and 16 ms. The $\pi/2$ pulse width, at -45^{o}C, is 4.5 $\pm$ 0.1 ms. This is not necessarily inconsistent with the room temperature measurement of 4.7 $\pm$ 0.1 ms, although it does suggest that the rf sensitivity may increase slightly as temperature decreases. If there is an increase in sensitivity, it would tend to increase the signal at low temperatures.

So, I took 64000 repetitions of 8 different contact times, as I did at room temperature, using the same 4.4 ms $\pi/2$ pulse (as there was no clear reason to change this, I left it as before). The data is, again, well described by equation 41. A gnuplot best fit, shown in figure 13, gives the values of I and $T_{1\rho}$ as 5.05 $\pm$ 0.07 $\cdot$ 10^{13} $\hbar$ $s^{-1/2}$ and 7.5 $\pm$ 0.9 ms, respectively. This is an increase of 36 $\pm$ 7%, in agreement with the 29 % predicted increase. This may also indicate a possible signal enhancement from the rf coil itself. The value of $T_{1\rho}$ is also consistent with that already found.

F. Longer contact time experiments

As I discussed in the theory chapter, the model I have been using is limited in accuracy to a few ms of contact time. A numerical model, that can be calculated given the measurements of I and $T_{1\rho}$, is presumed to better describe the evolution of the phosphorus spin polarization over contact times greater than $T_{1\rho}$. To check this, I extended my original experiments on sample 3 to include contact times up to 50 ms. Not surprisingly, I found that the simple decaying source model I have been using is inadequate. But, more curiously, although the behavior of the phosphorus spin polarization signal follows the form of my numerical model, there is significantly more spin polarization than should be accounted for.

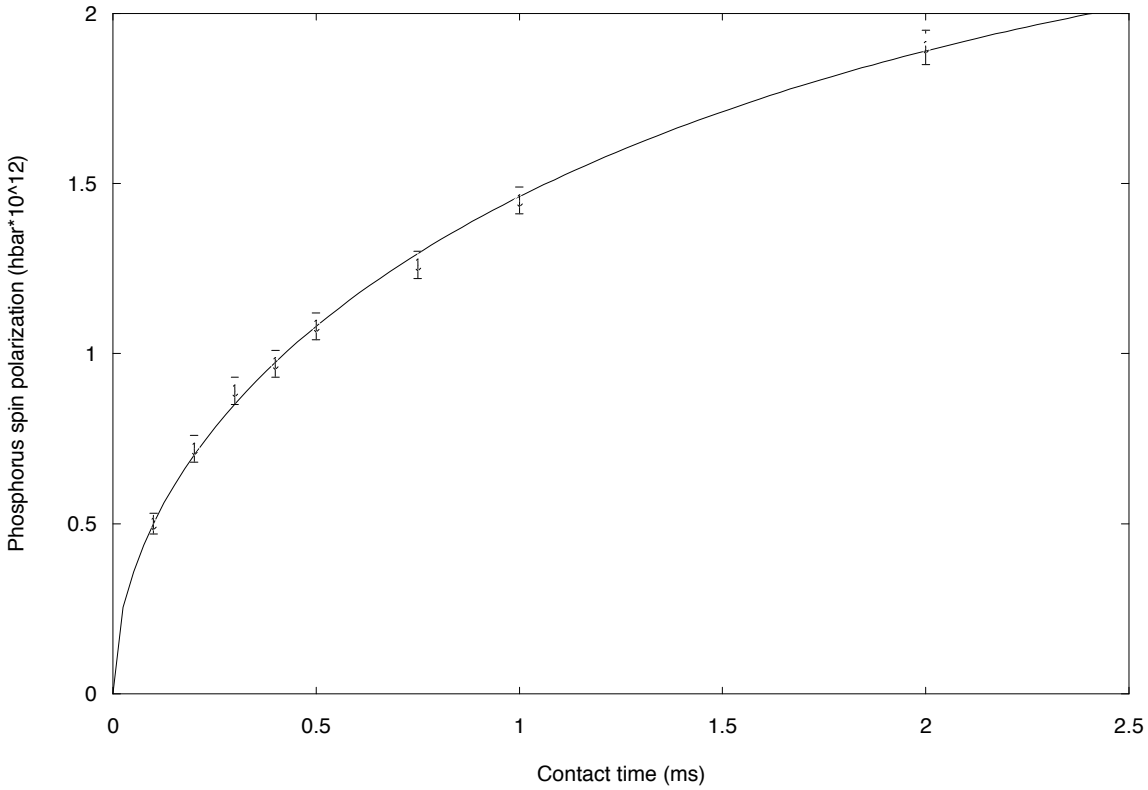

FIG. 13: Observed phosphorus spin polarization in sample 1, at low temperatures (T = -45^{o}C), versus contact time.

Figure 14 shows the results of my experiment, which also includes the relevant data for contact times below 2 ms, as previously measured, along with different model predictions. The numerical model, using $T_{1\rho} = 7.8$ ms, an intensity of $6.1 \cdot 10^{13}\ \hbar\ s^{-1/2}$, and the presumed diffusion constant of D=$3{\cdot}10^{-17}$ m^2/s is a much better fit than the that of equation 41, but it is still very far from the data. I found that, by dropping D down to $5{\cdot}10^{-18}$ m^2/s, I was able to get a significantly better fit. This fit still inadequately describes the decay of the phosphorus spin polarization. It also produces inconsistencies with my other results that confirm the size of the calculated diffusion constant. The fit has a reasonable shape, and shadows the decline of spin polarization quite effectively, but it still does not match the intensity.

The best solution may lie with toying with the other parameters in my numerical simulation. I found that my step sizes in the simulation are bordering on a critical size. If I increase D, Δt or Δx by even a factor of 3, the simulation breaks down, giving either negative or extremely large values of spin polarization. However, I am already working at the limit of

my computing abilities – Excel is already very slow at calculating the model, and gave me memory errors when I trebled the number of active cells. It may be that, just by decreasing the time and space step sizes, I may converge to a nicer fit. An alternative may be that more hydrogen contributes to the surface spin reservoir than just those in TFMBB directly attached to the InP grain. A layer of TFMBB a couple of molecules thick could increase the width of the hydrogen source. This would increase the amount of spin polarization flowing into the InP grain. I have not been able to fully investigate all of these possibilities.

One remaining possibility to explain these data lies in my assumption that spin diffusion is totally isotropic. I will show in my next experiment that the chemical shift of phosphorus in the surface atomic layer is a couple of KHz lower than the chemical shift of phosphorus inside the InP grains. As such, there will be a small energy difference between an oriented phosphorus spin in the surface layer, and an oriented phosphorus spin elsewhere in the InP grain. Thus, there could be a small effect that tends to inhibit spin diffusion back to the surface, once spin polarization has passed through the surface atomic layer. Even a slight inhibition would mean the phosphorus spin polarization would persist longer than predicted. This may explain the differences in spin polarization decays between my models and experiments.

The results of this experiment show that my modelling is on the right track for long contact times, although further refinement may be necessary to fully describe the situation. Considering that any of the presented curves are extrapolations to 50 ms, based on the initial 2 ms of data, the fact that they have any resemblance to the data does indicate that something is right with my model of the experiment.

G. Spin diffusion after cross-polarization

In several of my experiments I used a short delay between cross polarization and acquisition, to enhance my signal to noise ratio. During such a delay, the spin polarization of the phosphorus is allowed to diffuse inwards, into a region of homogenous chemical shift. Without a delay, the spin polarization is almost entirely in the surface atomic layer of the InP grains, whose NMR spectrum has a broad linewidth. In a series of experiments, varying the delay time in the xpbakup pulse program, I investigated the qualitative aspects of this broadening, and discovered a time dependant chemical shift does indeed indicate that the

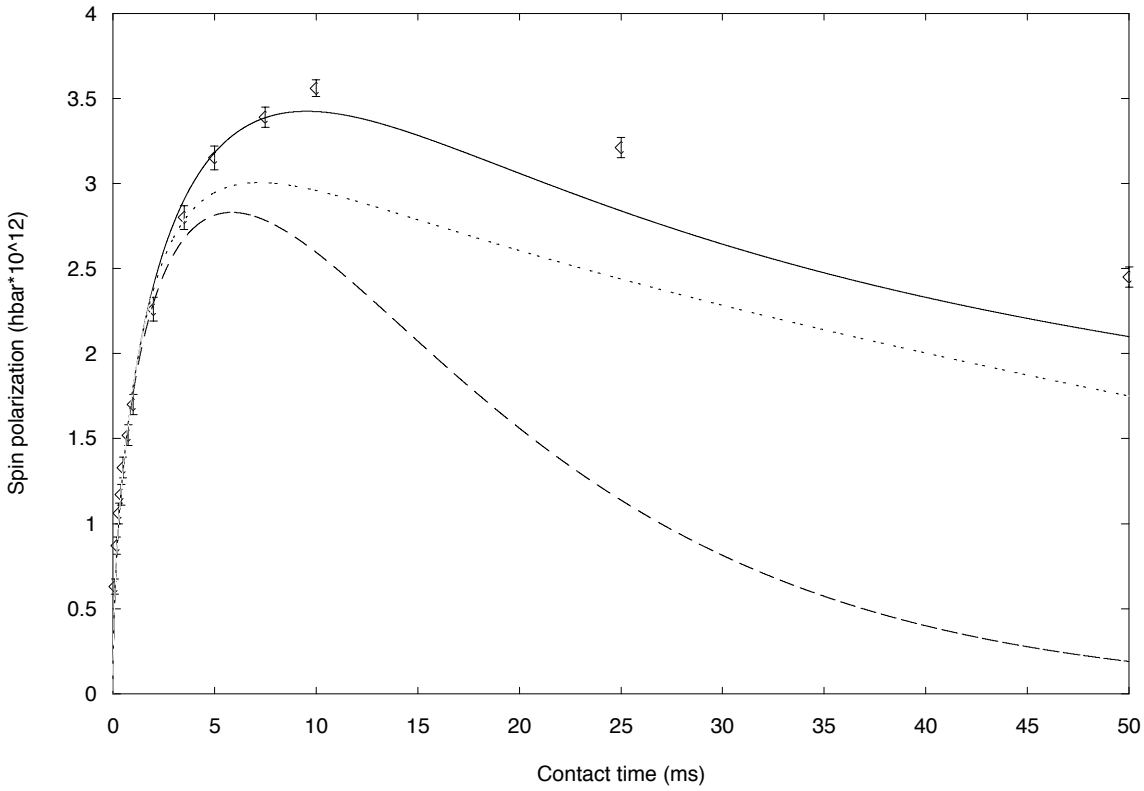

FIG. 14: Phosphorus spin polarization, as measured in sample 3 for long contact times. The dashed line is the prediction of equation 41. The dotted line is the prediction of the numerical simulation with D=$3{\cdot}10^{-17}$ m^2/s. The solid line is the same model, with D=$5{\cdot}10^{-18}$ m^2/s.

surface layer of phosphorus feels a very different, and much more varied, chemical shift than the phosphorus inside the grain. Indeed, one would expect that the surface atoms can see a wide variety of environments, from being adjacent to a hydrogen atom, to being several angstroms away from any.

Using 64000 trials, and otherwise optimized conditions, I measured the phosphorus signal in sample 1, with delays (parameter d3) from 0.01 s to 1.0 s, using the xpbakup program. I fit Gaussian peaks to the results, using Gnuplot, and have graphed the resulting fits in figure 15. One may notice several things from this graph. First, the width of the peaks shrinks as longer delays are included. Secondly, to conserve the area under the curve, and hence the total phosphorus spin polarization, the peaks grow taller as they decrease in width. Next, the chemical shift increases with longer delay times. I have shown this more clearly in figure 16, where the shift is explicitly graphed against the delay. I expect the phosphorus spin polarization to diffuse, on average, a distance $\sqrt{4Dt/\pi}$, as described in my

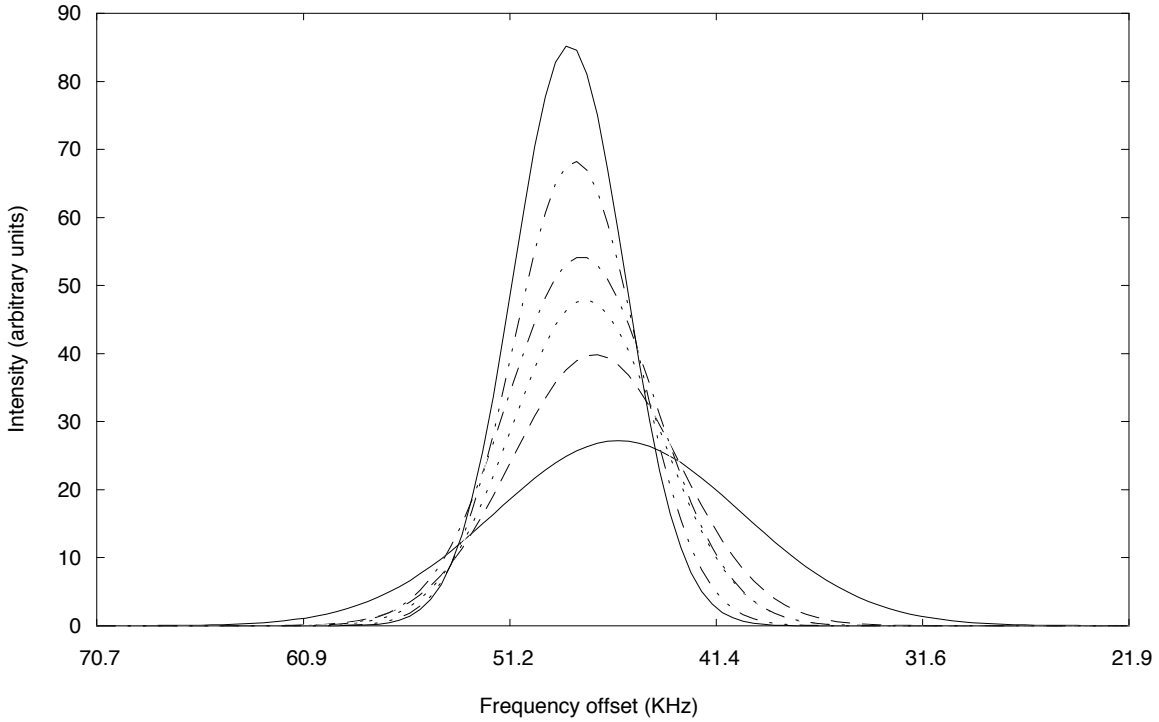

FIG. 15: Phosphorus spin polarization with delays before acquisition. Fits for d3 = 0.01, 0.1, 0.2, 0.3, 0.5, and 1.0 s, in ascending order of maximum intensity.

first model. If the average interatomic spacing is 3.7 $\mathring{A}$, and D = $3{\cdot}10^{-17}$ m^2/s, then it will take an average of 36 ms for spin polarization to diffuse out of the surface layer. This sets the timescale for the motion of the chemical shift. Looking at figure 16, it is apparent that about half of the change in chemical shift occurs in the first 100 ms, which is in reasonable agreement with what could be expected. Lastly, note that the left shoulder of all the fits, save that of the shortest time, are roughly the same, while the right shoulders are not. This is further evidence that most of the line broadening due to surface conditions lowers the chemical shift of the phosphorus.

To take this experiment further would have been interesting, but to extract quantitative results from it would require making substantial assumptions about the behavior of the chemical shift as a function of distance into the InP grain. As a continuation of my work, this experiment may offer the potential to measure the spin diffusion constant D.

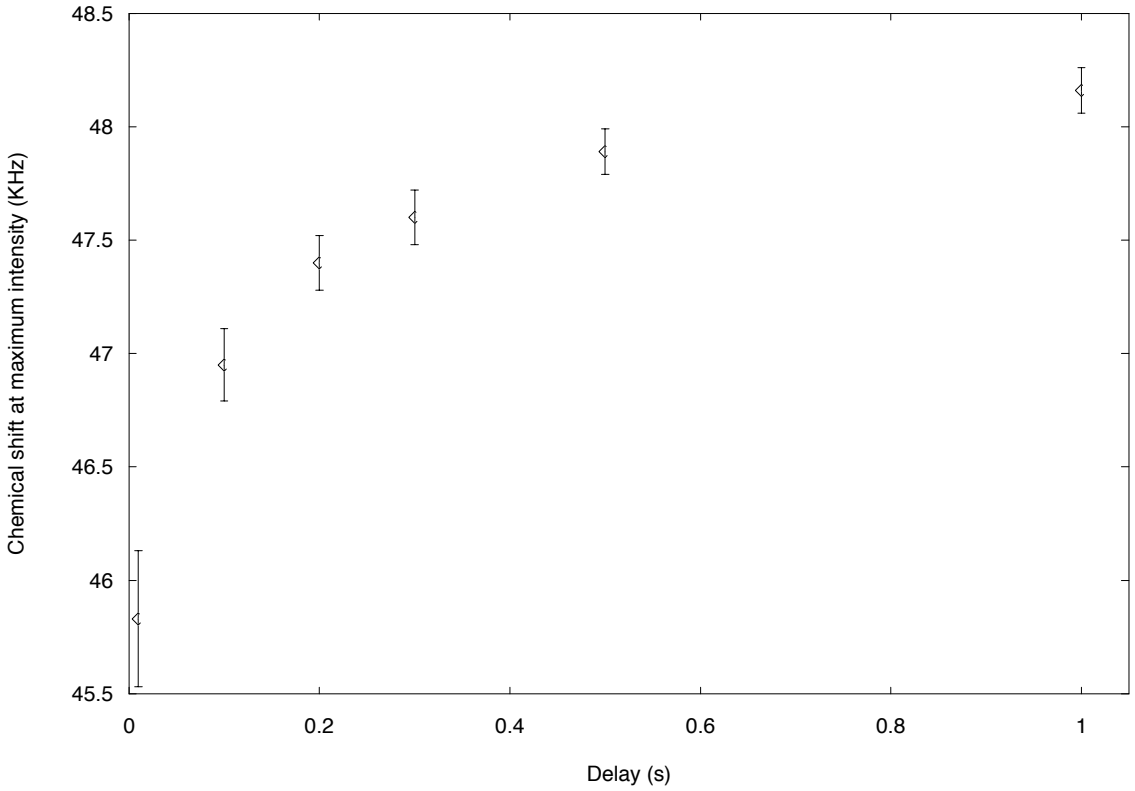

FIG. 16: Chemical shift of phosphorus signal as a function of acquisition delay.

H. Double contact experiments

The next experiment I did involved using the xp2 pulse program to move spin polarization from the hydrogen into the phosphorus, wait, and then return the spin polarization to the hydrogen. I used otherwise optimized conditions, but only allowed a 1 ms contact time for each cross-polarization phase. This allowed only a small amount of spin polarization into the phosphorus, which could then be treated as a point source for subsequent diffusion. The short cross-polarization returning spin polarization into the hydrogen was chosen to neglect relaxation effects, and to simply sample the surface spin polarization density of the phosphorus. I took data over several orders of magnitude of the delay, d3, during which phosphorus spin diffusion occurred. In my first experiment, I ran 32000 repetitions over the scale of 50 μs to 0.5 s. There was only interesting data in the last few data points, so I made two further attempts, going up to 3 s, to extend the range of data. Due to time constraints, I was only able to do 20000 repetitions of these long delay experiments. This led to very poor signal to noise ratios. Unfortunately, a key point, lying at 1.33 s, turned out to be unresolvable, although I managed to extract poor fits to a few longer delays.

I have been unable to find a reasonable explanation for these data, which are graphed in a log-log format in figure 17. The intuitive guess would figure that the spin polarization of the phosphorus would, for diffusion time scales longer than the initial cross-polarization, resemble a slowly expanding gaussian shape. This should have the spin polarization density at x = 0 as inversely proportional to its width, $\sqrt{4Dt/\pi}$. Thus, I would naively have expected that the hydrogen spin polarization should vary as $t^{-1/2}$, at least for diffusion times of greater than a few ms. This does not seem to be the case. I should reiterate a precaution I made when I presented my spin diffusion models – the assumptions behind my models are not appropriate for diffusion from a phosphorus source into an initially unpolarized hydrogen layer. Indeed, my attempted fits to variations of $t^{-1/2}$ are all very poor. I have plotted the data in a log-log format in order to attempt to bring light to the order of the dependence of the hydrogen signal to the delay d3. The signal intensity is roughly constant up till almost half a second, after which time it sharply declines. Based on the last three points, the data seem to fall with a slope of -2, implying a behavior asymptotic to t^{-2}. But, these data are not complete enough to clearly show the intermediate behavior. Also, this is a much more complicated experiment than I have been previously working with. As such, my analysis of this experiment will remain incomplete. More data, and some further refinement of my modelling of what's really going on is necessary.

It is comforting to note, however, that the timescale of the signal decay is about 0.1 to 1 s. This is in agreement with the previous experiment, that used chemical shifts to show that spin polarization moves away from the surface on a timescale of 0.1 to 1 seconds.

I. Direct hydrogen $T_{1\rho}$ measurement

Finally, I was able to use the flow of spin polarization to directly measure the hydrogen $T_{1\rho}$, a parameter that was previously extracted from my cross-polarization experiments as 7.8 ± .4 ms. I slightly modified the xpolar1 pulse program to include a hydrogen spin lock period before cross-polarization. I then allowed a brief, 1 ms cross-polarization to sample the hydrogen spin density at that time. I took 5 data points, from 1 to 20 ms of spin lock, with only 16000 repetitions at each point. The signal intensity is shown in figure 18. An exponential decay was fit to the data, giving the value of $T_{1\rho}$ as 11.0 ± 1.2 ms. This is similar to the measurement extracted from my other cross polarization experiments, but

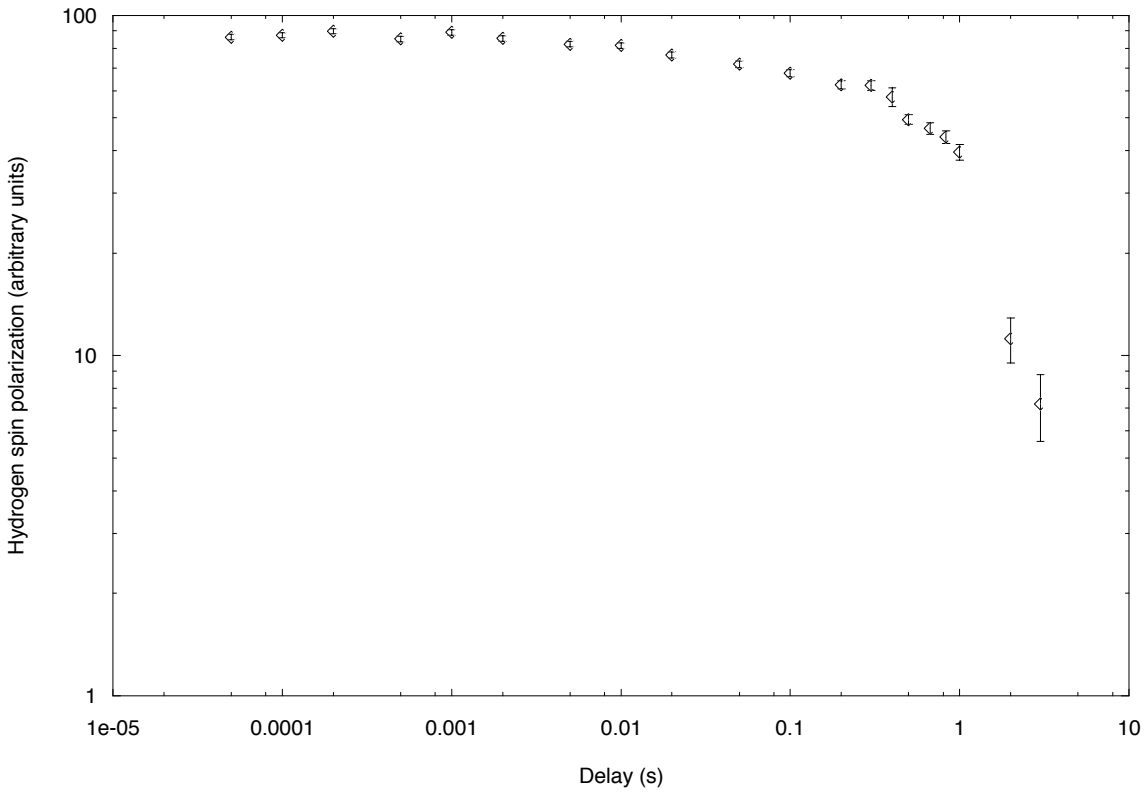

FIG. 17: Hydrogen signal intensity, as a function of delay time d3, on a loglog scale.

anomalously high.

The previous measurement was based on a model assuming the hydrogen spin density decays only via $T_{1\rho}$ relaxation. However, in reality, there is a drain on the hydrogen spin density through spin diffusion into the phosphorus. This will speed up the rate at which the hydrogen spin density decays. Since I neglected this effect, in order to make my model soluble, a fit to this model will measure a decay rate that includes both $T_{1\rho}$ relaxation, and the spin diffusion contribution. This will lead to an underestimation of the $T_{1\rho}$ relaxation time. Considering that up to one third of the hydrogen polarization may be transferred into the phosphorus, this underestimation could be significant enough to find my two different measurements of $T_{1\rho}$ in agreement.

VI. CONCLUSIONS

My proposed aim in observing, and quantifying the phenomena of spin diffusion between an organic molecule tightly bound to the semiconductor indium phosphide. I proposed a number of models, using basic assumptions, that attempt to describe what happens when

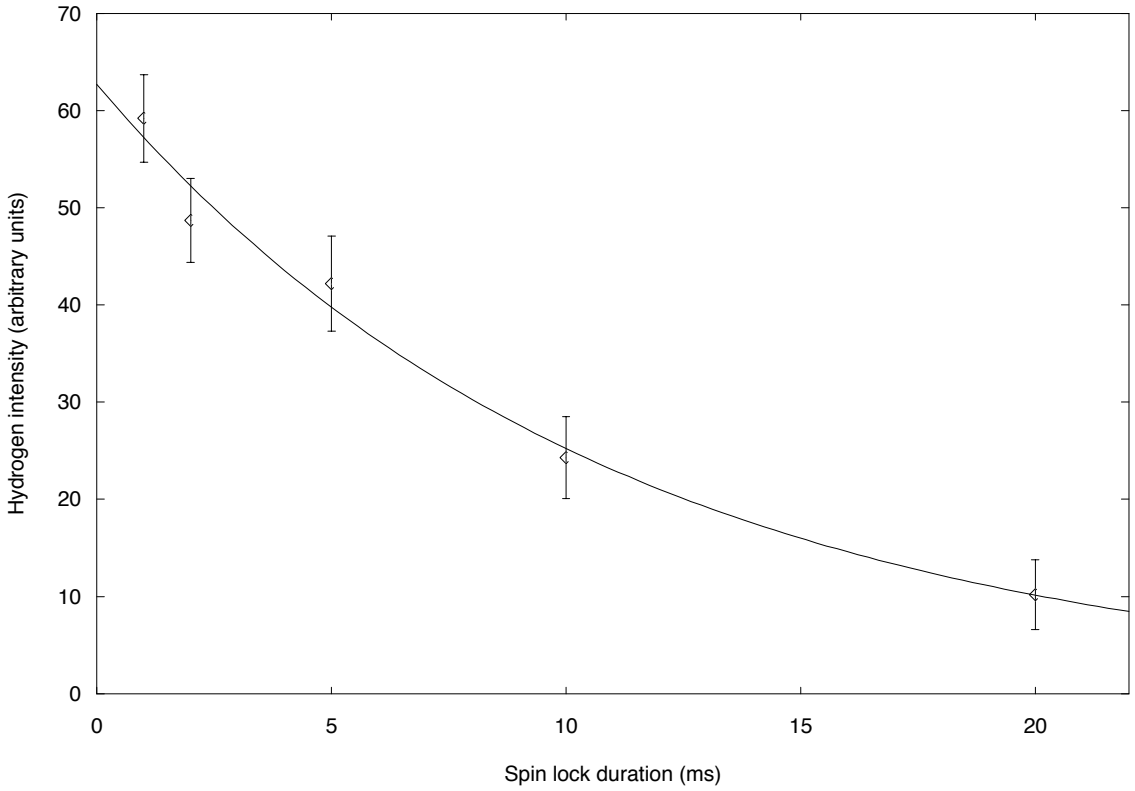

FIG. 18: Decay of hydrogen spin polarization by $T_{1\rho}$ relaxation in a spin lock field.

spin polarization flows from a surface source into a deep sink. These models, and considerations on the assumptions underlying them, may serve as a starting point for future work with optically enhanced spin polarizations.

In a series of experiments, I was able to optimize the Hartmann-Hahn cross-polarization condition, and calibrate the NMR probe to determine the absolute number of polarized nuclei in my sample. This calibration allowed me to check a number of predictions of my models. In simple situations, for short times, these predictions were found to agree splendidly with the data. In experiments where one, or more, of the basic assumptions behind my models were challenged, the behavior differed from these models. However, the manner in which data diverged from strained predictions may say something about certain parameters. In particular, while short contact time data is consistent with the theoretical prediction of the diffusion constant in InP, namely D = $3{\cdot}10^{-17}$ m^2/s, longer contacts suggested that D may be overestimated. However, the timescale set by observations of spin polarization moving away from the phosphorus surface layer are strong evidence that the calculated value of D is correct. Also, the decay of spin polarization in a spin locked field

undergoing cross-polarization was found to decay via a slightly modified $T_1\rho$. Finally, ϵ a fudge factor I introduced to describe the resistance of the organic-semiconductor interface to spin polarization under cross-polarization conditions, was found to be consistent with unity. This implies that spin polarization flows freely across the boundary, at least for tightly bound molecules. Indeed, a simple approximation suggests that up to a third of the initial hydrogen spin polarization eventually ends up in the phosphorus.

A number of other effects were observed within the study of cross-polarized samples, all of which are consistent with the qualitative understanding of the physical system. As spin polarization diffuses away from the surface, it undergoes a slight variation in chemical shift, and it finds the inner atoms of an InP grain to be more homogeneous than the outermost atomic layer. The cross-polarization signal intensity was found to increase with an increased initial hydrogen spin polarization density, and with increased surface area.

All these things suggest that future work in spin diffusion will have a successful base to build upon. This phenomena is observed to occur predicably, and efficiently enough to be of use when developing techniques for NMR signal enhancement through cross-polarization and optical pumping.

---

[1] E. Fukushima and S. B. Roeder, *Experimental Pulse NMR, a Nuts and Bolts Approach* (Addison-Wesley Publishing Company, Inc., Reading, Massachusetts, USA, 1981).

[2] L. J. Frank A. Bovey and P. A. Mirau, *Nuclear Magnetic Resonance Spectroscopy* (Academic Press, Inc., San Diego, California, USA, 1988).

[3] L. N. Hand and J. D. Finch, *Analytical Mechanics* (Cambridge University Press, Cambridge, UK, 1998).

[4] D. J. Griffiths, *Introduction to Quantum Mechanics* (Prentice Hall, Inc., New Jersy, USA, 1995).

[5] I. J. Lowe and S. Gade, Physical Review **156**, 817 (1967).

[6] C. P. Slichter, *Principles of Magnetic Resonance* (Harper and Row, Inc., New York, USA, 1963).

[7] A. G. Redfield and W. N. Yu, Physical Review **169**, 443 (1968).

[8] S. R. Hartmann and E. L. Hahn, Physical Review **128**, 2042 (1962).

[9] C. Michal, unpublished data (1998).

[10] M. Grinder, unpublished data (2002).